Remote Sensing of Environment 140 (2014) 350–364

Contents lists available at ScienceDirect

Remote Sensing of Environment

journal homepage: www.elsevier.com/locate/rse

Re-greening Sahel: 30 years of remote sensing data and field observations (Mali, Niger)

C. Dardel [a,*], L. Kergoat [a], P. Hiernaux [a], E. Mougin [a], M. Grippa [a], C.J. Tucker [b]

[a] Geosciences Environnement Toulouse (GET), Observatoire Midi-Pyrénées, UMR 5563 (CNRS/UPS/IRD/CNES), 14 Avenue Edouard Belin, 31400 Toulouse, France
[b] NASA Goddart Space Flight Center, Mail Code 610.9, Greenbelt, MD 20771, USA

ARTICLE INFO

Article history:
Received 12 June 2013
Received in revised form 5 September 2013
Accepted 12 September 2013
Available online xxxx

Keywords:
Sahel
Desertification
Re-greening
Trend analysis
Herbaceous production
NDVI
AVHHR
Field measurements
Mali
Niger

ABSTRACT

Desertification of the Sahel region has been debated for decades, while the concept of a "re-greening" Sahel appeared with satellite remote sensing data that allowed vegetation monitoring across wide regions and over increasingly long series of years (nowadays 30 years with the GIMMS-3g dataset). However, the scarcity of long-term field observations of vegetation in the Sahel prevents ground validation and deeper analysis of such trends. After assessing the consistency of the new GIMMS-3g NDVI product by comparison to three other AVHRR-NDVI datasets and MODIS NDVI, regional GIMMS-3g NDVI trends over 1981–2011 are analyzed. Trends are found positive and statistically significant almost everywhere in Sahel over the 1981–2011 period. Long-term field observations of the aboveground herbaceous layer mass have been collected within the Gourma region in Mali (1984–2011) and within the Fakara region in western Niger (1994–2011). These observations sample ecosystem and soil diversity, thus enabling estimation of averaged values representative of the Gourma and Fakara. NDVI measurements are found in good agreement with field observations, both over the Gourma and Fakara regions where re-greening and negative trends are observed respectively. A linear regression analysis performed between spatially averaged seasonal NDVI and a weighted average of field measurements explains 59% of the variability for the Gourma region over 1984–2011, and 38% for the Fakara region over 1994–2011. In the Gourma, which is a pastoral region, the re-greening trend is mainly observed over sandy soils, and attests for the ecosystem's resilience to the 1980s' drought, able to react to the more favorable rainfall of the 1990s and 2000s. However, contrasted changes in the landscape's functioning have occurred locally. An increase in erosion and run-off processes in association with decreasing or stable vegetation cover was observed over shallow soils, which occupy 30% of the area. In the agro-pastoral Fakara, the decreasing trends observed both from satellite NDVI and field assessments of herbaceous mass are hardly explained by rainfall. These results give confidence in the dominant positive trends in Sahelian greenness, but indicate that degradation trends can also be observed, both in situ and from satellite time series.

1. Introduction

Desertification of the Sahel has been debated for a long time within the scientific community (Aubreville & Chevalier, 1949; Hubert, 1920; Jones, 1938; Stebbing, 1935). The debates were refueled by the severe and regional droughts of the early 1970s (Boudet, 1972, 1977; Charney, 1975) and mid 1980s (Hein & de Ridder, 2006; Hellden, 1991; Hellden & Tottrup, 2008; Hulme, 2001; Le Houerou, 1996; Lindqvist & Tengberg, 1993; Nicholson, Tucker, & Ba, 1998; Prince, De Colstoun, & Kravitz, 1998; Prince, Wessels, Tucker, & Nicholson, 2007).

Desertification is defined by the United Nations as land degradation occurring in dry land caused by a range of factors including climate variations and human management. At the southern edge of the Sahara desert, the Sahel is particularly exposed to climatic fluctuations, and extreme events such as droughts or floods have severe consequences for the populations and their resources. In recent past the Sahel belt went through 25 years of below-average precipitations, starting in the early 1970s. Within this period, two particularly severe and regional scale droughts occurred in 1972–73 and in 1983–84 (Le Barbé & Lebel, 1997; Lebel & Ali, 2009; Nicholson, 2013; Nicholson & Palao, 1993). The impact of these droughts on the ecosystem was dramatic, however it should be distinguished from a desertification process in which impact on the ecosystem functioning has to be long-term. Furthermore, scaling issues rapidly emerge when local soil degradation has to be put in the broader perspective of a potential widespread desertification.

With the arrival of spaceborne remote sensing data in the 1970s, global monitoring of vegetation has become possible. Various vegetation indices and statistical methods have been used to monitor vegetation "greenness" in time and space. The GIMMS dataset, produced by the NASA Global Inventory Modeling and Mapping Studies group from the series of Advanced Very High Resolution Radiometer (AVHRR) sensors (Tucker et al., 2005) is widely used. Although these sensors were not initially designed to capture vegetation signature, a vegetation

* Corresponding author. Tel.: +33 5 61 33 29 32.
E-mail address: cecile.dardel@get.obs-mip.fr (C. Dardel).

0034-4257/$ – see front matter © 2013 Elsevier Inc. All rights reserved.
http://dx.doi.org/10.1016/j.rse.2013.09.011

index based on the red and infrared spectral bands proved very efficient for vegetation monitoring and is particularly used for analyzing global and regional trends and variability. The first analyses of NDVI trends over the west African region indicated a general increase of the vegetation index, which was interpreted as a "re-greening" of the region (Anyamba & Tucker, 2005; Eklundh & Olsson, 2003; Fensholt, Rasmussen, Nielsen, & Mbow, 2009; Herrmann, Anyamba, & Tucker, 2005; Heumann, Seaquist, Eklundh, & Jonsson, 2007; Olsson, Eklundh, & Ardo, 2005). These results fed the controversy between a Sahel suffering from desertification and a "re-greening" Sahel (Hutchinson, Herrmann, Maukonen, & Weber, 2005). It was also argued, according to satellite data, that the Sahara desert was in fact not expanding southwards (Tucker, Dregne, & Newcomb, 1991; Tucker, Newcomb, & Dregne, 1994; Tucker & Nicholson, 1999).

A number of studies first characterized the "re-greening" trends and then attempted to analyze possible factors such as rainfall distribution, soil type and soil cover, or plant phenology (de Jong, de Bruin, de Wit, Schaepman, & Dent, 2011; Fensholt & Rasmussen, 2010; Fensholt et al., 2012; Herrmann et al., 2005; Heumann et al., 2007; Huber, Fensholt, & Rasmussen, 2011; Olsson et al., 2005; Seaquist, Hickler, Eklundh, Ardo, & Heumann, 2009; Townshend & Justice, 1995). Two types of greening were evidenced: in northern Sahel re-greening trends were attributed to an increase of the NDVI amplitude (annual cycle), while in southern Sahel they were related to an increase of the growing season duration (Eklundh & Olsson, 2003; Fensholt et al., 2009; Olsson et al., 2005).

As new satellites directly designed for vegetation monitoring were launched, more datasets have become available with finer spatial and spectral resolutions providing very valuable tools, but they cannot substitute the 30 year-long archive needed in long-term trends analysis. Several versions of the same original AVHRR data have been produced: the PAL (James & Kalluri, 1994), GIMMS (Tucker et al., 2005), LTDR (Pedelty et al., 2007), and now GIMMS-3g datasets differ in terms of calibration, atmospheric corrections and compensation for orbital drifts. The differences between these datasets in terms of NDVI trends over West Africa were analyzed (Beck et al., 2011; Fensholt, Sandholt, & Stisen, 2006; Fensholt, Sandholt, Stisen, & Tucker, 2006), and it was shown that the GIMMS NDVI dataset was the most suitable for temporal changes analysis, while the LTDR V3 dataset performed best in terms of absolute values despite residual calibration issues, as demonstrated by the presence of consistent trends of NDVI over desert areas (Beck et al., 2011). Because the GIMMS-3g NDVI dataset has just been released, studies assessing its consistency with the other NDVI datasets are not available yet, but it is increasingly used (Zhu et al., 2012 and other articles in the special issue).

However, because of difficulties to obtain high-quality data with sensors not originally designed to monitor vegetation, but also because of the uncertain relationship between spectral radiance measured from space and ecosystem structure and functions, the Sahel desertification/re-greening debate is not solved yet. To our knowledge none of these studies could refer to long-term vegetation ground observations to validate or help interpreting satellite observations. Very few long-term networks exist worldwide, and field observation networks in Sahelian regions proved very difficult to install and manage throughout long time periods. This is precisely the main contribution of the present study: analyzing NDVI data together with field observations of vegetation collected over a network of sites in the Gourma region in Mali over 28 years, from 1984 to 2011 (Hiernaux, Mougin, et al., 2009; Mougin et al., 2009), and in the Fakara region in western Niger over 17 years, from 1994 to 2011 (Hiernaux, Ayantunde, et al., 2009). While the Gourma region is located in pastoral Sahel, the Fakara is an agro-pastoral region with about half of the landscape being under shifting cultivation with a dynamic land use history. The Gourma and Fakara regions thus provide particularly contrasted study areas.

The questions this study aims to answer are the following:

i. What are the NDVI trends observed over the Sahel over the last three decades? Are the different NDVI datasets in agreement? How sensitive are the computed NDVI trends to the time period considered?
ii. What trends are observed with field observations of herbaceous vegetation in Gourma and Fakara?
iii. Are NDVI and field observations trends in agreement?
iv. How can these NDVI trends be interpreted?

2. Data and methods

2.1. NDVI datasets

Three of the NDVI datasets analyzed in this study were produced from data collected with the AVHRR sensors onboard the National Oceanic and Atmospheric Administration (NOAA) polar orbiting meteorological satellite series: LTDR, GIMMS and GIMMS-3g. The Normalized Difference Vegetation Index (NDVI) is calculated from the AVHRR channel 1 (red, 550–700 nm) and channel 2 (near-infrared, 730–1000 nm). The MODIS NDVI products from Terra and Aqua (MOD13C2 and MYD13C2) were also used for comparison over the recent 2000–2011 period.

The GIMMS-3g dataset has the longest period of observation and is increasingly used (Zhu et al., 2012, and other articles in the special issue). Therefore, after assessing its overall consistency by comparison to the other NDVI datasets, it is the basis of the present trend analysis.

2.1.1. GIMMS NDVI dataset

The GIMMS NDVI dataset is available from 1981 to 2006 with a spatial resolution of 8 km. Channel 1 and channel 2 LAC (Local Area Coverage, 1 km) reflectances are processed into GAC (Global Area Coverage, 4 km) data by averaging four out of five LAC pixels in a first line, then skipping the two next lines (Kidwell, 1998). The GAC pixels are assigned to the output grid (8×8 km) by a forward transform mapping using the satellite pixel center to determine the corresponding output cell. NDVI maximum value composites are then computed to compensate for the lack of cloud screening (Holben, 1986). The calibration happens in two steps. First, channel 1 and channel 2 reflectances are calibrated by the Vermote and Kaufman technique (Vermote & Kaufman, 1995). Then the NDVI is adjusted with the technique of Los (1998) using desert areas as calibration targets. To compensate for the sensors orbital drift and produce a consistent long-term NDVI record despite the use of several AVHRR sensors (Table 1), artificial trends have to be removed from the surface signature. The empirical mode decomposition technique (Pinzon, Brown, & Tucker, 2005) is applied, which minimizes solar zenith angle effects by removing the bias due to variable solar zenith angles as a function of sensor drift. The GIMMS NDVI has no atmospheric corrections, except for the volcanic eruptions of El Chichon (1982) and Mt Pinatubo (1991): stratospheric aerosol corrections are made for 1982–1984 and 1991–1994. Aggregated SPOT Vegetation data are used to perform the intercalibration between the NOAA-14 and NOAA-16/17 sensors, and the GIMMS NDVI is produced to be consistent with the dynamical range of SPOT-VGT and MODIS data.

The navigation accuracy obtained by coastal border check is about ± 1 pixel, which is good as far as global and regional analysis are concerned but may be insufficient when a pixel by pixel analysis is considered in continental areas. In the present study, navigation corrections were applied using tie-points on several sites in West Africa with invariant NDVI over time such as some lakes and rocky areas. A correction of $+0.057°$ in longitude and $-0.068°$ in latitude was applied regionally.

2.1.2. GIMMS-3g NDVI dataset

The GIMMS-3g NDVI dataset is the latest version of the GIMMS NDVI produced by the NASA Global Inventory Modeling and Mapping Studies

Table 1
NOAA satellites used to produce the GIMMS and GIMMS-3g NDVI datasets.

Instrument	NOAA-7	NOAA-9	NOAA-11	NOAA 9-d	NOAA-14	NOAA-16	NOAA-17	NOAA-18	NOAA-19
Dates of coverage	Jul. 1981–Feb. 1985	Feb. 1985–Sept. 1988	Sept. 1988–Aug. 1994	Aug. 1994–Jan. 1995	Jan. 1995–Nov. 2000	Nov. 2000–Dec. 2003	Dec. 2003–Jul. 2005	Jul. 2005–Apr. 2009	Apr. 2009–present

group. It is available from July 1981 to December 2011, with a spatial resolution of 1/12° and bimonthly composite images. This version was processed to provide better quality data for the high latitudes than the previous dataset. Calibration was performed using SeaWifs data instead of SPOT Vegetation data (Zhu et al., 2012). As for the GIMMS dataset, navigation precision was checked out in our study area. No systematic shift was observed and no navigation correction was applied.

2.1.3. LTDR NDVI dataset

The Long-Term Land Data Record project is conducted by NASA Goddard Flight Space Center and was designed to produce land climate related datasets by merging data from the AVHRR sensors from 1981 to 1999 with MODIS data from 2000 up to today (Pedelty et al., 2007). Daily reflectance, NDVI, and quality assessments are produced with a spatial resolution of 0.05° which matches the MODIS Climate Modeling Grid (CMG). LTDR version 3 was used in this study with reprocessed AVHRR GAC data over the 1981–1999 period. The GAC reprocessing includes pre-processing improvements (channels 1 and 2 in-flight calibration, inverse navigation to improve navigation) and atmospheric corrections used in the MODIS processing. Rayleigh scattering and water vapor content are corrected for using NCEP (NOAA Center for Environmental Prevision) outputs, ozone content is obtained from TOMS (Total Ozone Mapping Spectrometer) and aerosol correction is applied. LTDR consistency is monitored over several AERONET sites as well as over “golden tiles” constituted of 50 km × 50 km subsets distributed over sites characterized by different vegetation types.

2.1.4. MODIS NDVI datasets

The MODIS NDVI product MOD13C2 is based on data from the Terra satellite, while the MYD13C2 NDVI product is based on data from the Aqua satellite. Aqua has an equatorial crossing time in the afternoon (1:30 pm) while Terra has an equatorial crossing time in the morning (10:30 am).

The MOD13C2 product is available from 2000 onwards at a 5.6 km (0.05°) spatial resolution and a monthly temporal resolution (Justice et al., 1998, 2002). It is obtained from temporal and spatial averages of the MOD13A2 NDVI product (1 km, 16 days), which is in turn based on the daily surface reflectance product (MOD09). The MOD09 red and infrared surface reflectances are corrected for the effect of atmospheric gases and aerosols. The MYD13C2 product has the same spatial and temporal characteristics. It is computed through the same scheme, and is available from 2002 onwards.

2.2. Field observations of vegetation

2.2.1. Mali (Gourma region)

The Gourma region is located in north-eastern Mali and covers approximately 90,000 km^2 to the south of the Niger River. The region considered in this study and referred to as the “Gourma window” covers 30,000 km^2 and extends from latitude North 14.5° to 17.5° and from longitude West 0.8° to 2.2° (Fig. 1). Field observations of vegetation were collected from 1984 to 1999 by Hiernaux & Diarra (ILRI, International Livestock Research Institute; Hiernaux & Turner, 1996) and from 1999 to 2011 within the African Monsoon Multidisciplinary Analysis (AMMA)—Couplage de l'Atmosphère Tropicale et du Cycle Hydrologique (CATCH) observatory (Hiernaux, Mougin, et al., 2009; Mougin et al., 2009). The Gourma region covers a bioclimatic gradient where precipitations range from 150 mm/year in the northern edge to 400 mm/year in the southern edge. The landscape is composed of about 65% deep sandy soils, 30% shallow soils and 5% loamy-clay soils. The Gourma is a pastoral region where less than 5% of the surface is cultivated. The vegetation cover mainly consists of annual herbaceous plants, while woody plants occupy on average less than 3% of the surface. Therefore, the vegetation variable used in this study is the aboveground standing mass of the herbaceous layer as a proxy for vegetation aboveground production. However, the database also provides meteorological data, complementary data on herbaceous vegetation (cover, height, plant density, standing litter, root mass, species composition), soil type (texture profile, organic matter and nutrient contents), grazing pressure intensity, and woody plant population (Hiernaux, Diarra, et al., 2009; Hiernaux, Mougin, et al., 2009).

The sampling strategy was designed to be representative at the landscape scale, the objective being to build a dataset compatible with the 1 km resolution of the LAC AVHRR remote sensing data. Therefore, observations and measurements were made on 30 homogeneous sites of 1 km^2 (1 m wide by 1 km long lines) distributed along the bioclimatic gradient in the main landscape units as defined by topography, water system, soil types, land use and grazing pressure intensity (Fig. 1).

In order to account for spatial heterogeneity, the sampling of herbaceous vegetation with site is performed through a two level stratified random sampling (Hiernaux, Mougin, et al., 2009). Major heterogeneity related to topography or soils is dealt with distinguishing facieses, while local heterogeneity in herbage masses is dealt with distinguishing four strata within each facies: bare soil (nil or close to nil vegetation cover), low, medium and high density. The frequency of the facieses and strata is read, meter per meter, along the 1 km-long transect. Measurements of herbaceous mass are performed by destructive cutting, drying and weighing on a set of plots randomly selected within each stratum: 6, 6 and 12 plots for the low, high and medium density strata respectively. The total herbaceous mass of the site is then computed by weighting the mass measured for each stratum by the stratum frequency. Several measurements per year are generally available, but for this study the maximum value for each year has been employed. End of season observations of annual plants is considered a good proxy for annual aboveground productivity in this biome (Le Houerou, 1984; Sala & Austin, 2000). Rainfall data from the Hombori Synoptic Meteorological station are used to interpret vegetation trends.

2.2.2. Niger (Fakara region)

The Fakara region is located in southwestern Niger and covers approximately 6000 km^2 between the Niger River and the Dallol Bosso valley. The region considered in this study and referred to as the “Fakara window” covers 500 km^2 and is centered on the district of Dantiandou (latitude North 13°24′57″, longitude East 2°45′2″, Fig. 2). The climate is semi-arid with a mean annual precipitation of about 500 mm with high spatial and temporal variability (Le Barbé & Lebel, 1997). The Fakara landscape is a highly fragmented agro pastoral land with a very dynamic land use. Indeed, a large increase in land area under cultivation occurred over the last decades (Hiernaux & Turner, 2002) and frequent shifts happen between fallowing and cropping. Woody plants cover about 5% of the landscape in average and are mostly composed of sparse trees and diversely dense shrubs (Hiernaux & Ayantunde, 2004). As for the Gourma region, this study mostly focuses on the herbaceous õvegetation mass variable.

Field observations of vegetation began in 1994 with an ILRI project aiming to assess fodder resources (Hiernaux & Ayantunde, 2004), and continued since 1999 within the AMMA-CATCH observatory (Cappelaere et al., 2009). The end of season herbaceous mass

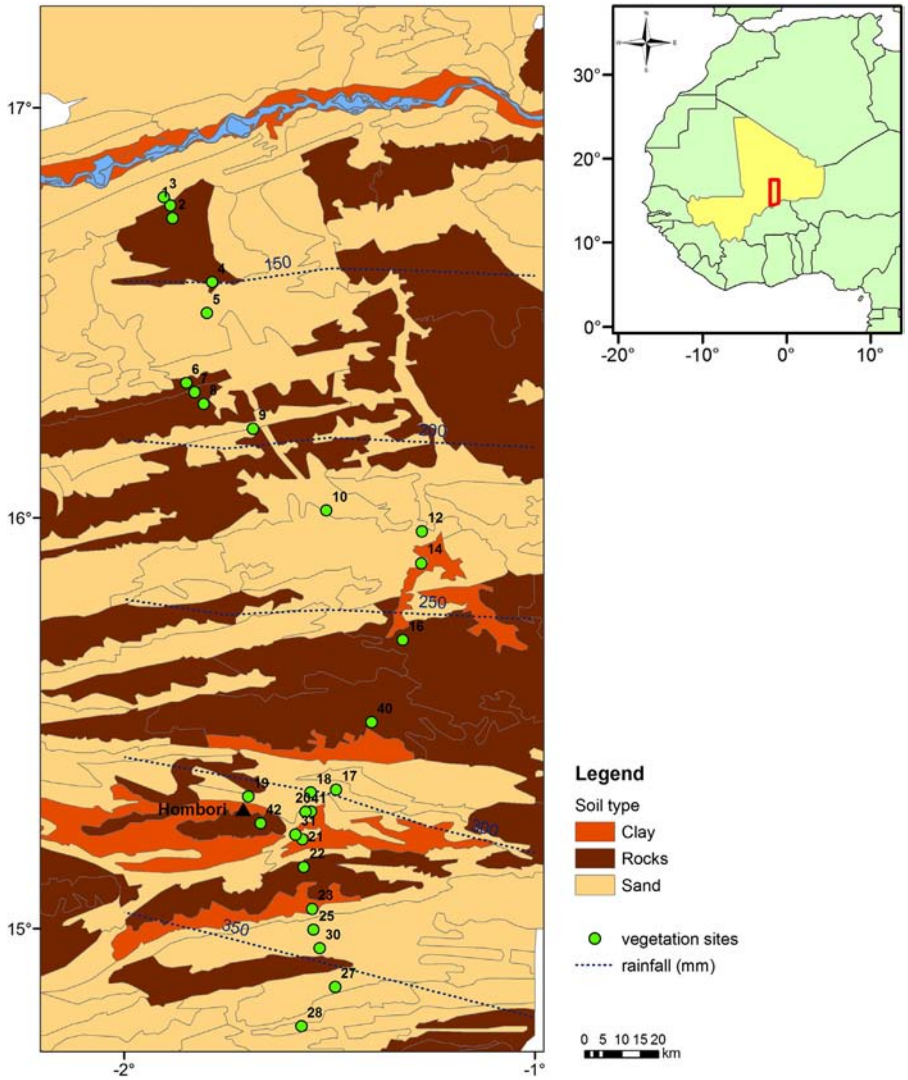

Fig. 1. Study area in Gourma (Mali) with vegetation survey sites and dominant soil type.

(October) is used as the estimate of herbaceous annual production. The vegetation dataset aims at sampling the main topographic situations, soil types, and land use types, based on a set of 24 sites (12 crops, 12 fallows–rangelands) monitored over years. Because of the frequent shifts between cropping and fallowing and to ensure equilibrium between the numbers of cropped and fallowed/rangeland sites, sites were continuously added to the initial dataset, so that since 2006, the 24 sites are selected every year in a pool of 72 historical sites (Hiernaux, Ayantunde, et al., 2009). Production is estimated for rangelands, fallows (old, recent, new) and cropped fields (low, medium, high density, and manured fields) in the main landscape units (plateau, sandy soil slopes, valleys).

In fallow and rangeland sites, the sampling strategy applied is the same two level stratified random sampling and destructive measurement used for the Gourma observations (see Section 2.2.1), except that measurements are made along 200 m-long transects, to account for the size of fields.

In cropped fields, the mass of weeds is determined by following the same destructive method, the only difference being that 10 plots are selected every 10 m along a 100 m-long transect and no stratification is performed. Indeed, crops are regularly weeded so that the weeds density can be considered randomly distributed. The mass of cropped plants is estimated by determining their density by a distance method named Point Centered Quadrant method (PCQ) applied every 10 m along the 100 m-long transect. The PCQ method consists in measuring the distance of the nearest crop plant to the sampling point within four quadrants defined as the intersection of the transect and its perpendicular. These four distances are averaged at each sampling point, and plant density is computed based on the average of these distances using the density algorithm (Cottam & Curtis, 1956). At each of the sampling points, a millet plant is sub sampled and its mass measured. Finally, grain mass is indirectly estimated using a harvest index and added to the total mass of the millet crop. Rainfall data from the Niamey Square degree (average of 29 Synoptic Meteorological stations located in the Niamey super site, see Lebel & Ali, 2009) are used to interpret vegetation trends.

2.3. Methods

2.3.1. NDVI temporal average

NDVI is related to the quantity of photosynthetically active plants and is known to be a good estimator of vegetation properties such as green leaf area index (LAI), green vegetation cover fraction (fCover), fraction of absorbed photosynthetically active radiation (fAPAR), and primary production (Myneni, Hall, Sellers, & Marshak, 1995; Myneni & Williams, 1994; Tucker, 1979). NDVI is commonly used to monitor herbaceous vegetation changes in Sahel (Tucker, Justice, & Prince, 1986; Tucker, Vanpraet, Sharman, & Van Ittersum, 1985). Net primary production is estimated by averaging the 15 day NDVI composites over August and September, equivalent to integrating the NDVI curve over that period of main growth.

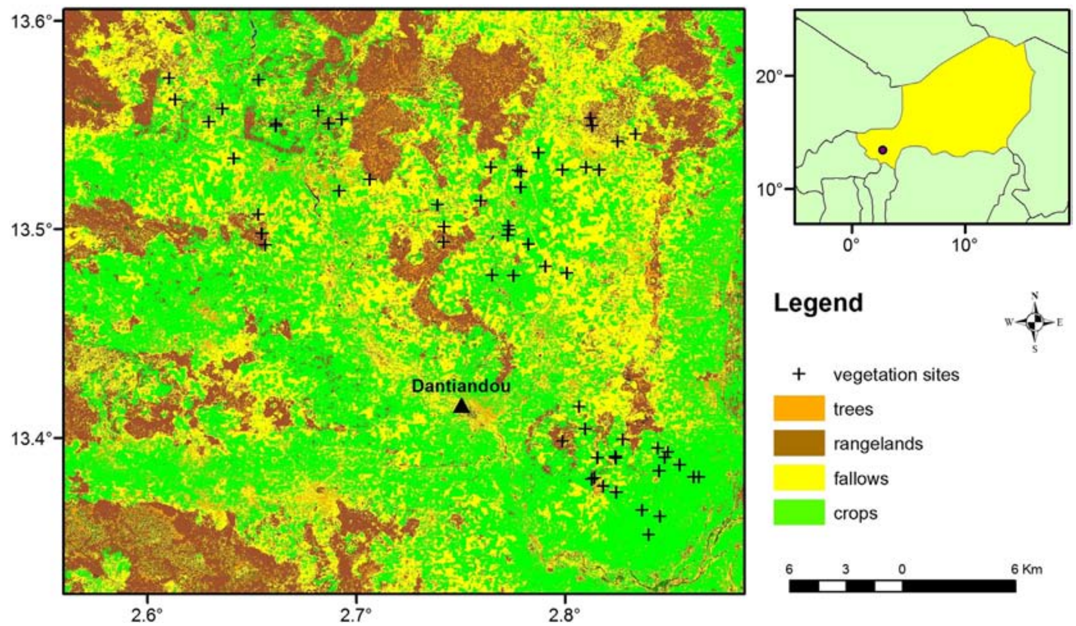

Fig. 2. Study area in Fakara (Niger). Vegetation survey sites are plotted onto the land cover map. The supervised classification was performed from a LANDSAT image from October 2007.

Preliminary work was performed to determine the method and time period to use for computing "annual" NDVI values: averaging different months, or integrating after removing the dry season NDVI value, see Mbow, Fensholt, Rasmussen, and Diop (2013) for instance. The results obtained with each method were fairly close in terms of trends maps, interannual variability and comparison to field observations. We selected the simple "average method" for the August and September months, which catch most of the herbaceous vegetation dynamics both in rangelands and croplands in our study regions, is widely used in literature (Anyamba & Tucker, 2005; Fensholt et al., 2009; Hellden & Tottrup, 2008; Tucker et al., 2005) and is easily reproducible.

2.3.2. NDVI datasets intercomparison

In order to test the consistency of GIMMS-3g with the other datasets, maps of correlation over time were computed for GIMMS-3g/GIMMS (1981–2006), GIMMS-3g/LTDR (1981–1999) and GIMMS-3g/MOD13C2 (2000–2011). Maps of correlation were also computed for GIMMS-3g/MYD13C2 and MOD13C2/MYD13C2 over 2002–2011 (not shown).

Linear regressions were computed on a per pixel basis over the Sahel region. The spatial resolution being different among products, the coordinates of the pixel center of the dataset with the finer resolution were used to select the closest pixel of the other dataset. Areas where the correlation is not significant at the 95% level are masked out (in light gray on maps). Similarly, areas where NDVI standard deviation over time is below 0.015 NDVI units are masked out (in dark gray on maps), the NDVI signal being too low to enable interpretation (these areas are mainly located in the Sahara desert).

To assess the interannual variability consistency of the GIMMS-3g dataset, temporal profiles were examined as well. Spatial averages were performed over the Gourma and Fakara windows (see Sections 2.2.1 and 2.2.2).

2.3.3. NDVI trend computation

Linear regressions were computed on a per pixel basis to produce regional maps of GIMMS-3g NDVI trends over 30 years (1981–2011) over the Sahel region and over the Gourma and Fakara windows. Slope values multiplied by the number of years are subsequently referred to as the "linear increment". Significance threshold is set at 95%. Areas where this threshold is not reached are masked out as well as areas where NDVI standard deviation is below 0.015 NDVI units.

When studying trends over time, a key question remains the sensitivity of trends to the time period considered within the 30 year-long series: the start and end years can have tremendous impacts on the sign or strength of the computed trend. Thus, linear increments and associated p-values were computed systematically, for every possible time period between 1981 and 2011.

2.3.4. NDVI comparison to field observations

2.3.4.1. Trend comparison and correlation analysis. Because of the scale differences between field data and the 1/12° satellite pixels, NDVI data and field measured herbaceous masses were spatially aggregated. GIMMS-3g NDVI seasonal mean values were spatially averaged over the windows described in Sections 2.2.1 and 2.2.2. A weighted average of in-situ measurements was computed to provide one time series per study area representative of the Gourma and Fakara windows, as described in Sections 2.3.4.2 and 2.3.4.3. Linear trends were computed for each dataset with time as the independent variable. A linear correlation analysis and a Spearman rank correlation were performed between the spatially aggregated time series of NDVI and herbaceous layer mass.

2.3.4.2. Weighted average of field observations, Gourma (Mali). The landscape of the Gourma region is composed of three main units: deep sandy soils, shallow soils on hardpan or rock outcrops, and fine textured soils (clayed) in low lands. The respective proportions of each of the main landscape units within the Gourma window were estimated as 65.1% of sandy surfaces, 30.8% of shallow soils, and 4.1% of clayed depressions (see Fig. 1). These proportions were used to weighted average herbaceous mass values of sites grouped by soil type, in order to obtain a unique time series directly comparable with satellite data. Comparison was made to a raw average of field observations over all sites and results were similar (not shown).

Although it is not the best method due to the size of the GIMMS-3g pixels, NDVI was extracted for the nearest pixel of each field site (consistency was checked out by analyzing temporal profiles for the 8 surrounding pixels, not shown) and averaged following the soil type attribution. Linear correlations between the three classes of NDVI and field data (sandy, shallow and clayed soils) were computed and shown for information.

2.3.4.3. Weighted average of field observations, Fakara (Niger). The 48 sites observed each year in the Fakara region sample the landscape heterogeneity but disregard the proportions of the landscape units. Thus, to perform the comparison with spatially aggregated NDVI data within the window previously described, field data were averaged using two successive weightings.

First, the relative extent of rangelands, fallows and cultivated areas estimated through supervised classification performed on high resolution imagery (Table 3) are used to weight mean herbaceous masses per land use type. Land use being very dynamic in Fakara, this weighting evolved over time: fallows and cropland changed significantly, whereas area of rangelands was considered constant. The overall accuracy was found to be 84.5% for the 1986 classification (Kappa coefficient = 0.76), 91% for the 2008 classification (Kappa coefficient = 0.86) and 84.4% for the 2011 classification (Kappa coefficient = 0.78). The crop class is particularly well distinguished from the other classes.

Then further weighting was performed for croplands as four categories of cropland were sampled, based on crop density: low, medium, high and very high in manured crop fields. From previous field surveys and mapping the relative extent of the categories is estimated at 60% low density, 24% medium density, 8% high density and 8% manured crops respectively all along the period (no significant changes were observed). These proportions were used as weights to estimate the overall (crops plus weeds) herbaceous mass of croplands.

3. Results

3.1. NDVI datasets comparison

3.1.1. Regional analysis

Good overall agreement is found among all datasets over the Sahelian belt (Fig. 3). Results over the Sahara region were masked out (light gray) because of a too sparse or nil vegetation cover (NDVI under the 0.015 threshold). Correlation values are also low over the sub-humid Sudanian belt where the NDVI signal may be saturated at peak growth and may be contaminated by frequent clouds. The higher correlation coefficients over the Sahel belt are found between the LTDR and GIMMS-3g NDVI datasets (and also between the two MODIS NDVI products, not shown). GIMMS and GIMMS-3g are also significantly correlated (over 1981–2006 as shown on Fig. 3b and over 1981–1999, not shown), while the correlation is weaker for GIMMS-3g/MODIS MOD13C2 (11 years only). A slightly higher correlation is found between GIMMS-3g and MYD13C2 (Aqua) over 2002–2011 (not shown), most probably due to the similar equatorial crossing time (during the afternoon both for MODIS Aqua and the AVHRR sensor).

Such an overall agreement, when focusing over the Sahel belt, allows the use of GIMMS-3g NDVI data to compare with field measurements over the longest possible time period.

Table 2
Linear regressions between the different NDVI datasets over the Gourma and Fakara regions. The correlation is computed with the first indicated dataset as the dependant variable (e.g. GIMMS-3g/LTDR means GIMMS-3g = f(LTDR)). Correlations over 1981–1999 were added for the 3 longest datasets for comparison purposes.

NDVI datasets	Time period	Linear regression	Gourma (Mali)	Fakara (Niger)
GIMMS-3g/GIMMS	1981–2006	r^2	0.88	0.9
		Slope value	0.59	0.64
	1981–1999	r^2	0.99	0.94
		Slope value	0.65	0.64
GIMMS-3g/LTDR	1981–1999	r^2	0.92	0.73
		Slope value	0.68	0.65
GIMMS/LTDR	1981–1999	r^2	0.89	0.75
		Slope value	1.02	1
GIMMS-3g/MOD13C2	2000–2011	r^2	0.88	0.7
		Slope value	1.22	0.75

Table 3
Relative extent of crops and fallows over the Fakara region estimated from supervised classifications performed on high resolution imagery.

Year	1986	2007	2008	2011
Crops (%)	25.3	37.4	42.5	48.9
Fallows (%)	52.1	36.7	35	31.2

3.1.2. Temporal profiles

The five NDVI temporal profiles averaged over the Gourma and Fakara windows display a good consistency, especially in terms of trends and interannual variability (Fig. 4 and Table 2). Processing differences (atmospheric effects correction, sensors intercalibration…) and also band width differences with MODIS explain the shift in NDVI absolute values. The GIMMS dataset in particular displays absolute values lower than the three other products. GIMMS-3g is in good agreement with the LTDR product over 1981–1999 and with the MODIS MOD13C2 and MYD13C2 products over 2000–2011 and 2002–2011 respectively. All products show below-average NDVI values during the 1983–84 drought, and above-average peaks in 1994 and 1999, two years which correspond to higher than average rainfall (Lebel & Ali, 2009).

A linear correlation shows that MOD13C2 explains 88% of the variability in the GIMMS-3g dataset for the Gourma region (Fig. 5a) and 70% for the Fakara region (Fig. 5b). The correlation coefficients found for the regression between GIMMS-3g and MODIS MYD13C2 over 2002–2011 are lower (79% for the Gourma and 66% for the Fakara; not shown).

3.1.3. Phenology

Over the Gourma window and over the whole 1981–2011 period, GIMMS-3g NDVI trends computed for each month are positive and significant for August, September and October, i.e. during the growing season peak (Fig. 6a). This implies that, in this region, positive NDVI trends can be mostly interpreted as an increase in NDVI amplitude (Heumann et al., 2007). Negative significant trends are observed during the dry season, and even at the beginning of the rainy season (April to July), which is most probably due to artifacts. Indeed, GIMMS-3g NDVI trends over 1981–2000 do not show such negative trends for these months (Fig. 6b), while they appear when trends are computed over 2000–2011 (Fig. 6c), but not for the MODIS MOD13C2 dataset (Fig. 6d). The same patterns were found over the Fakara region (not shown). Given that we compute annual values of NDVI by averaging NDVI from August to September, this does not impair the following results.

3.2. NDVI trends analysis

3.2.1. Regional GIMMS-3g NDVI linear trends

GIMMS-3g NDVI trends over the Sahel are widely positive and significant except in a few spots, the larger negative patterns being found over western Niger, central and eastern Sudan (Fig. 7a). Anywhere else, positive trends i.e. re-greening trends are observed. Highly contrasted patterns, strongly positive and negative, are found over the Gourma and Fakara windows respectively (Fig. 7b).

3.2.2. Sensitivity of trends to the time period

In the two-dimensional parameter diagram (Fig. 8), years with above average NDVI are characterized by particular patterns: a strong green vertical line meaning that the aforementioned year has greater NDVI values than the previous ones, and a strong red horizontal line meaning that the following years are characterized by lower NDVI values. Similarly, years with below average NDVI are clearly identifiable in the diagram: the impact of the 1983–84 drought is obvious with a red patch for the years of the droughts and strong positive trends for all time periods starting in 1983 or 1984.

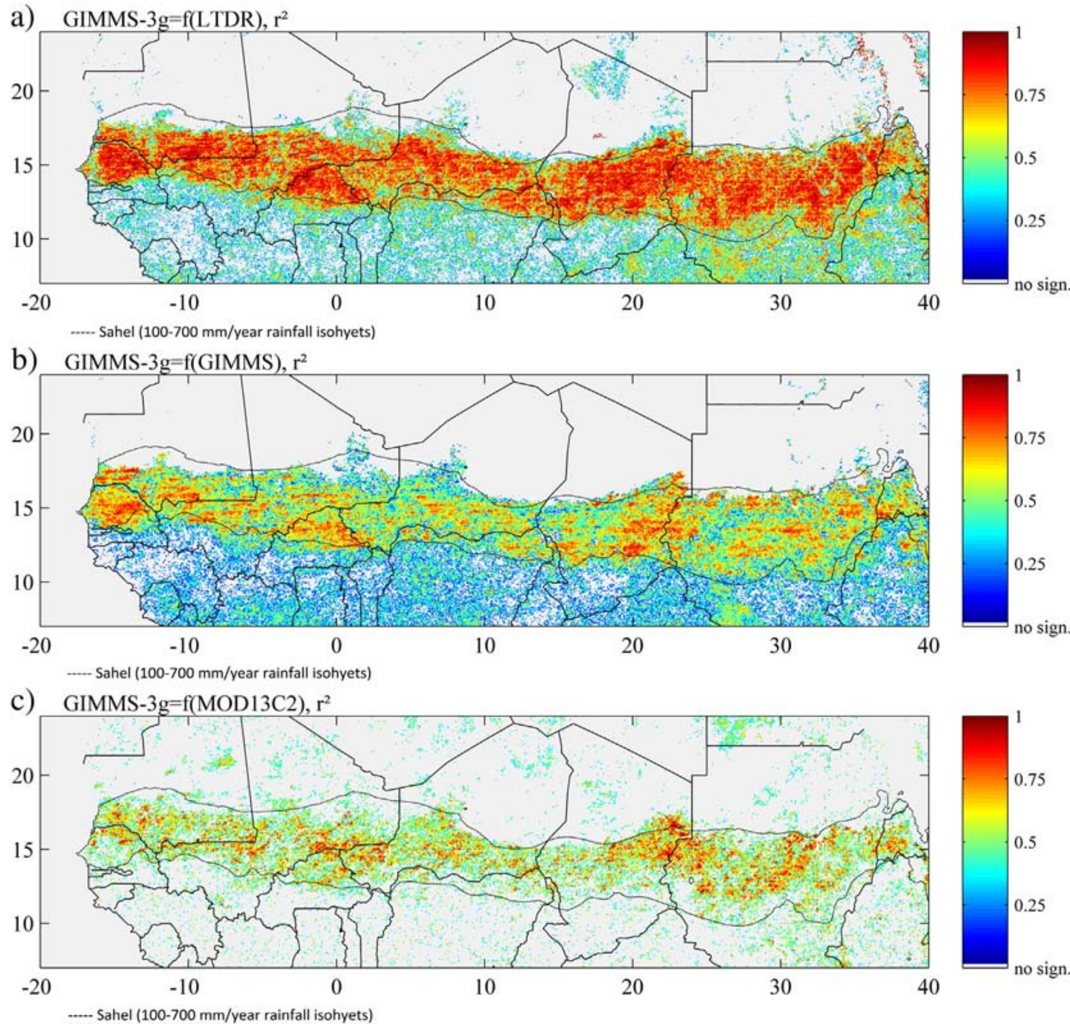

Fig. 3. Maps of square correlation coefficient of the linear regression between: a) LTDR/GIMMS (1981–1999), b) GIMMS/GIMMS-3g (1981–2006), and c) MOD13C2/GIMMS-3g (2000–2011). Significance threshold is set at 95% (areas masked out in gray).

In the Gourma window, trends beginning in the mid 1980s are positive and statistically significant for all time periods (Fig. 8a and b). Negative trends are found for time periods starting in the late 1990s, but few of them are statistically significant. On the contrary 1994 and 1999 appear to favor strong positive NDVI trends as well as 2010 and 2011. Thus, the NDVI trends computed over the Gourma window are mostly significant re-greening trends for almost every time period following the 1983–84 drought.

In the Fakara window, first the same re-greening trends after the 1983–84 drought are observed (Fig. 8c and d): trends are positive for time segments starting in the mid 1980s and going up to the mid 1990s, but the associated significance levels are rather low. After that period, negative trends become widely dominant and more significant: a very strong negative pattern is found for time segments starting around 1994 and ending in 2011. Similar patterns are observed for time periods ending in the last three years, suggesting that NDVI was still decreasing in 2009, 2010 and 2011. Therefore, according to satellite data, vegetation cover in Fakara seems to have constantly and strongly decreased after a short recovery stage following the 1983–84 drought.

3.3. NDVI comparison to field observations

3.3.1. Gourma region

Annual herbaceous vegetation masses measured in the field show a positive and significant linear trend over the 1984–2011 period, both the raw (not shown) and weighted averages (Fig. 9a). The linear increment reaches 589 kg DM ha^{-1} for the weighted average (p-value < 0.002) and 686 kg DM ha^{-1} for the raw average (p-value < 0.001). The NDVI trends, computed considering all years or only years when field observations are available, are both positive and significant (Fig. 9b). The slightly lower linear increment of the longest series (0.032 instead of 0.05) is mainly due to 1981 and 1982, the two years preceding the drought.

Both the field and satellite datasets show low values in 1984, 1985–1987, 1992–1993, 1995, 2004, and 2008 and high values in 1999, 2010 and 2011. However, some disagreement is found for 1988 and 1989, where herbaceous mass values stand higher than what the NDVI values would suggest.

A linear correlation between the NDVI series and the weighted average of field observations shows that GIMMS-3g explains 59% of the interannual variability in in-situ measurements (Fig. 9c). The Spearman rank correlation is 0.74.

3.3.2. Trend analysis by soil type

The GIMMS-3g NDVI trends as a function of soil types over the Gourma window (compare Figs. 1 and 7b) indicate positive significant NDVI trends over the large sandy soil areas and over the clay-dominated areas, while no significant trends are observed over shallow soils. In fact, the larger shallow soil units even display negative trends, but these are masked out (gray shading) because they are not significant.

Temporal profiles of field observations classified into the three categories (sandy, shallow, clay) (Fig. 10a) confirm that re-greening trends

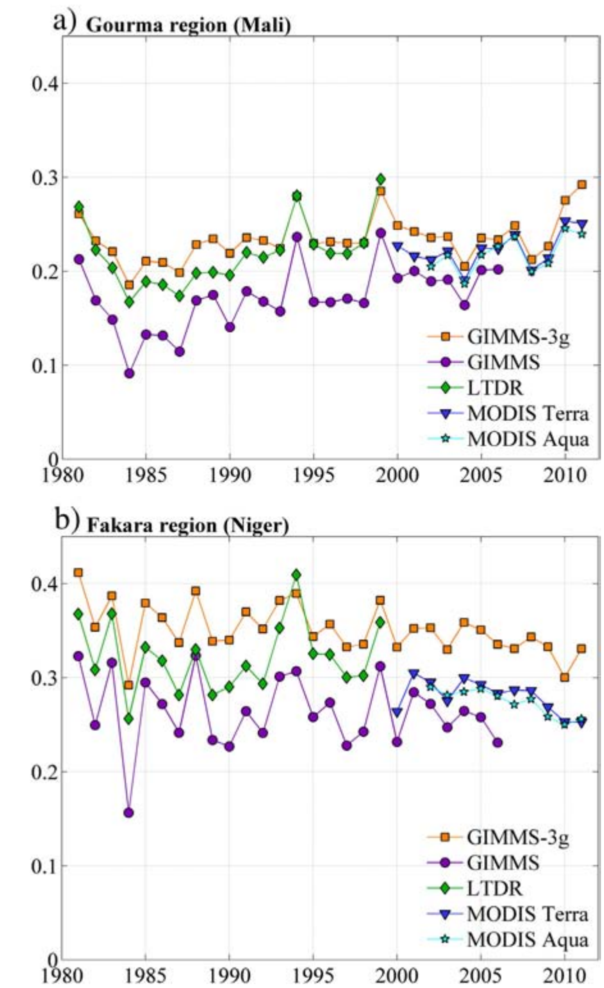

Fig. 4. NDVI temporal profiles over a) the Gourma region and b) the Fakara region.

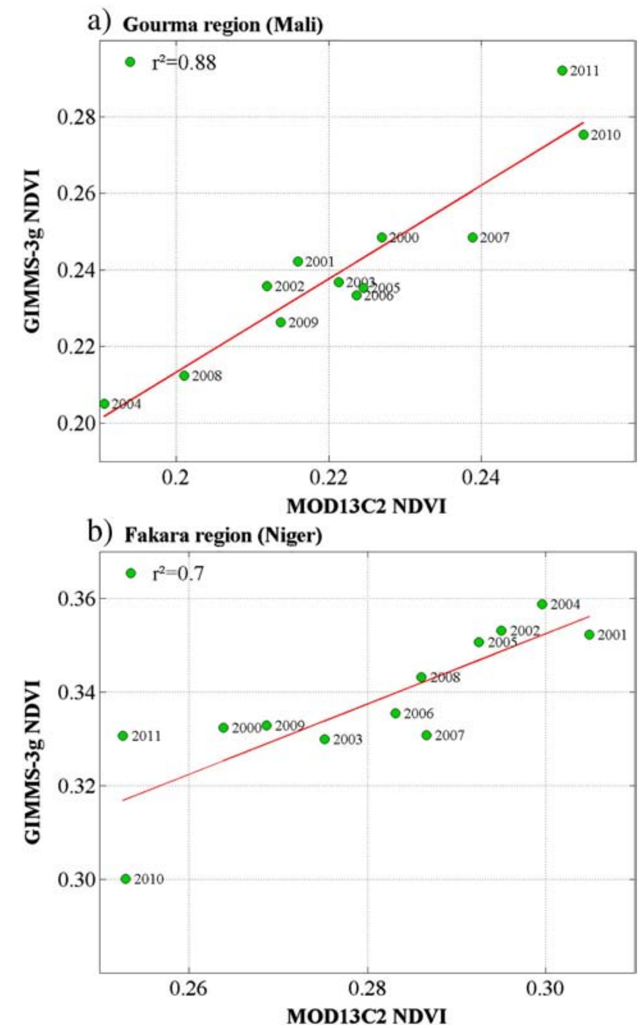

Fig. 5. Linear regression between GIMMS-3g and MODIS Terra NDVI over a) the Gourma region and b) the Fakara region.

are observed on sandy soils: the linear increment of field measurements reaches 769 kg DM ha^{-1} over the whole period (1984–2011) with a p-value of 0.017. These sandy soil sites are most of the time homogeneous at the GIMMS-3g pixel scale. The correlation at the pixel scale is good ($r^2 = 0.68$ with a p-value > 0.001, Fig. 10b) and the trends over time are comparable.

In low land sites with clayed soils, field observations show a very high positive trend of herbaceous mass (linear increment of 1372 kg DM ha^{-1}, p-value of 0.005), which is in part due to an increase in run-on over the period (Gardelle, Hiernaux, Kergoat, & Grippa, 2010; Timouk et al., 2009). Correlation with NDVI is poor ($r^2 = 0.24$, p-value = 0.014) due to the small size of clayed units: the satellite pixels covering a larger area than the typical scale of a clayed soil site, vegetation is observed over a mixed pixel including other soil types, which have changed differently over time.

Field observations over shallow soil sites show a positive slope value which is low (210 kg DM ha^{-1} over the period with a p-value of 0.048) and is in fact mainly due to 2010 and 2011. Without these two years, the trend is not significant anymore and is much lower (linear increment of 89 kg DM ha^{-1} with a p-value of 0.37). As shown before, vegetation yield was particularly high in 2010 and 2011 over the entire Gourma. Thus, small sandy or loamy patches encountered among wide rocky or hardpan outcrops bore higher vegetation cover. Correlation with NDVI is poor ($r^2 = 0.25$, p-value = 0.014) due to low vegetation yields at the pixel scale, which are difficult to assess with accuracy with satellite data.

3.3.3. Fakara region

NDVI and field observations trends in Fakara over the overlapping period (1994–2011) are both negative and statistically significant (Fig. 11a and b). The field observations linear increment reaches −336 kg DM/ha (p-value of 0.1), while the GIMMS-3g NDVI linear increment equals −0.04 NDVI units. When computing a linear correlation between field herbaceous mass values (weighted average) and seasonal GIMMS-3g NDVI averaged over the Fakara window, GIMMS-3g explains 17% of the variability in in-situ observations. However, the year 2010 is found to significantly differ from the regression line as well as from the regression between MODIS and GIMMS-3g (Fig. 5b). As similar uncertainties regarding the end of the GIMMS-3g dataset were reported (Zhu et al., 2012), we chose to analyze the relationship between NDVI and field measurements over Fakara with and without considering 2010. When not considering 2010, GIMMS-3g explains 38% of the variability in in-situ observations (Fig. 11c). The Spearman rho coefficient (rank correlation) is 0.41 when considering all years and 0.59 without 2010.

4. Discussion

4.1. NDVI trends over Sahel and comparison to field observations of the herbaceous layer mass

The positive and significant GIMMS-3g NDVI trends observed over most parts of the Sahel reinforce the hypothesis of a global Sahelian

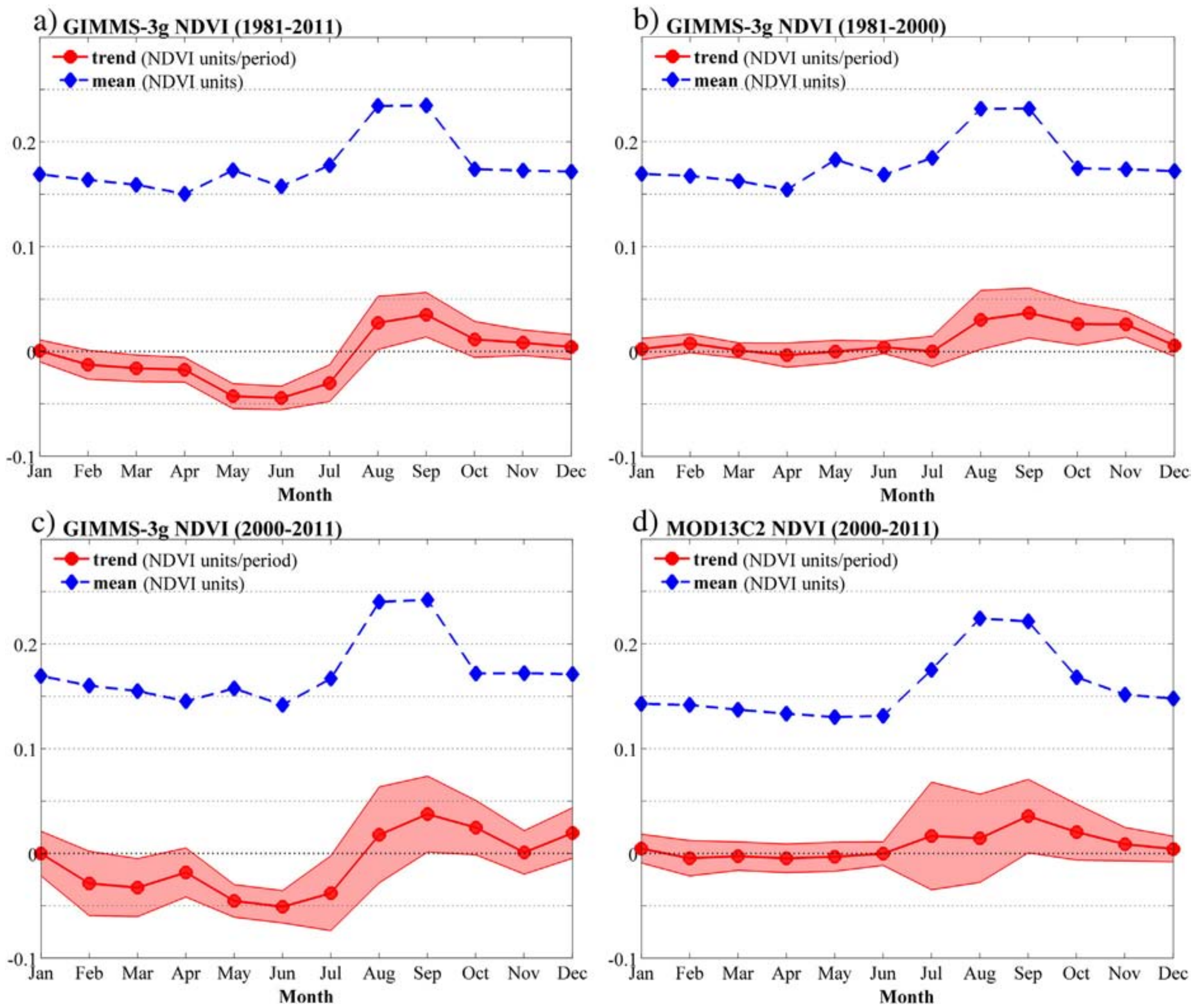

Fig. 6. NDVI averaged over the Gourma window: seasonal cycle is displayed in blue (dotted line) while the linear increments for each month of the year (for instance, the trend for January NDVI over the whole period) are shown in red (plain line). The pink shadow is the 95% confidence interval. a), b), c) show the GIMMS-3g NDVI trends for 1981–2011, 1981–2000 and 2000–2011 respectively, while d) shows the results for MODIS Terra NDVI over 2000–2011. (For interpretation of the references to color in this figure legend, the reader is referred to the web version of this article.)

re-greening occurring since the 1980s (Anyamba & Tucker, 2005; Eklundh & Olsson, 2003; Fensholt et al., 2009; Herrmann et al., 2005; Heumann et al., 2007; Hickler et al., 2005; Olsson et al., 2005) and further establish that the trends are maintained even when a longer period is considered. Only a few spots in the Sahel show significant negative NDVI trends, the more important negative patterns being found in western Niger, central and eastern Sudan.

In the Gourma region, the strong re-greening pattern, strengthened by the sensitivity analysis to time period, suggests a high resilience of the ecosystems after the 1980s' drought. In the Fakara region, a recovery behavior similar to the one observed over the Gourma region is found in the years following the drought, but a significant and constant decline in NDVI is observed since the mid 1990s that is not explained by rainfall, as shown by the above-average rainfall recorded on the same time period (Fig. 12). Not surprisingly, the period considered for the trend analysis is therefore critical, and multi-decadal time series of ground and satellite data are very valuable to outline and interpret significant trends.

There is ample literature on the accuracy of the relation between NDVI and Aboveground Net Primary Production (ANPP) or end-of-season biomass, including studies in the Sahel starting as early as 1985 (Tucker et al., 1985). Typically, when several years and several sites are considered, correlation coefficients range from $r^2 = 0.6$ to 0.7 (Diallo, Diouf, Hanan, Ndiaye, & Prevost, 1991; Hiernaux, 1988; Prince, 1991; Tucker et al., 1985). Few studies, however, evaluate such relationships over decades, because long-term productivity series are scarce and also because the comparison to NDVI requires demanding sampling or upscaling strategies. In front of such a lack of data, studies tend to use proxies such as tree rings or crop yield statistics. A notable exception (An, Price, & Blair, 2013) found remarkably similar statistics ($r^2 = 0.53$) for NDVI/ANPP linear relation over 17 years in central US tall grass prairie.

Let alone the issues encountered in the NDVI dataset itself, the relationship between NDVI (either integral, average or maximum over a period) and ground-measured vegetation mass is limited by uncertainty in the relationship between NDVI and absorbed radiation, in the conversion of absorbed radiation in net primary production, and in the links between production and end of season biomass. Soil effects on NDVI (background color, texture), grazing pressure (lowering end-of-season measured standing herbaceous mass but not necessarily annual production), floristic composition, or land use and farming methods are potential sources of variability, and may have changed when several decades are considered.

As an example, field sampling and upscaling are more complex in the case of agro-pastoral Fakara than pastoral Gourma. As land use is very dynamic, interannual variations of the respective proportions of each land use class should be followed. A small part of the landscape is constituted of manured crops, which have much higher productivity than the other cropped fields. Thus, small variations from year to year in the proportions of manured crops can affect the overall herbaceous production and the correlation between NDVI and field measurements if not accounted for.

In this study we have shown that variability and trends in NDVI time series are well explained by the trend in herbaceous mass in the Gourma, and consistent with the same trend in the Fakara. The good relationship found between NDVI data and field observations of the herbaceous mass highlights that NDVI is particularly well correlated to the herbaceous layer productivity in the Sahel, even when long-term archives are used. It proves that vegetation trend analysis using long-term satellite data is not only possible, but that satellite archive is an effective and reliable tool, both for qualitative and quantitative studies.

4.2. Trends interpretation

4.2.1. Rainfall

Rainfall is the first driver of vegetation production in Sahel (Penning de Vries & Djitéye, 1982). In the Gourma region, the re-greening trends evidenced can be related in the first order to rainfall trends over the last three decades. As an example, anomalies of annual rainfall measured at the Hombori meteorological station exhibit a linear increment of 109 mm over 1981–2011 (p-value = 0.08; see Fig. 12a). However, the negative trends found in vegetation production over the Fakara window both with ground measurements and satellite data are hardly explained by trends in annual rainfall. Indeed, rainfall measurements collected over the Niamey Square Degree do not exhibit significant trends (linear increment of 39 mm over 1990–2011, p-value = 0.50; linear increment of −58 mm over 1994–2011, p-value = 0.43; see Fig. 12b). Other factors should be taken into account to interpret trends and will be discussed later on.

4.2.2. Soil type and changes in landscape

In the Gourma region, significant positive trends in both NDVI and field observations are mainly observed over sandy surfaces and clayed depressions. On the contrary, the positive trend is very weak over shallow soils and only significant when including the two last years of the time period (2010 and 2011), during which rainfall were exceptionally high. Large increase in run-off has occurred during the past decades over the shallow soil sites in Gourma as in other Sahel regions (known as the "Sahelian paradox", Descroix et al., 2009), in some places in association with vegetation decay and strong erosion, which shows up on high resolution satellite data or aerial pictures (Descroix et al., 2012; Gardelle et al., 2010). As a consequence, more water runs on in the low lands where the vegetation cover increases.

Therefore, even in a region like Gourma where an overall re-greening trend is indisputable, changes may occur in the ecosystems and in some hydrological processes which can have important impacts on the landscape functioning. Local degradation trends are thus actually happening as demonstrated by the large increase in erosion processes and run-off rates and the vegetation decline over shallow soils. Observations of such phenomena (vegetation decline over some areas coupled to increased run-off and vegetation cover in other areas) may help reconciling the re-greening and degradation theories.

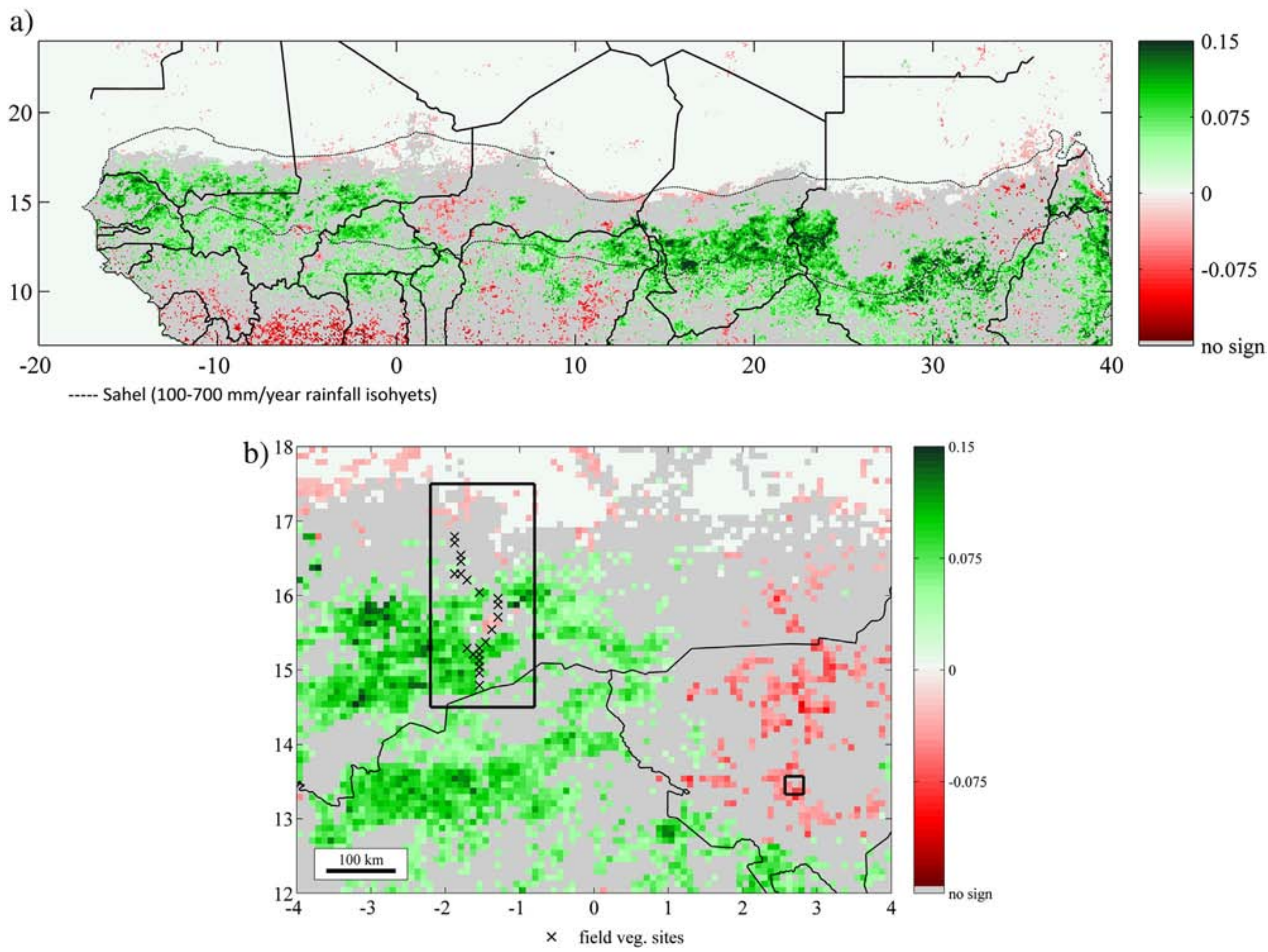

Fig. 7. a) GIMMS-3g NDVI trends (linear increment) from 1981 to 2011 over the Sahel region. Dark gray areas are not significant at the 95% level, while areas where NDVI standard deviation is lower than 0.015 NDVI units are masked out in light gray. b) Zoom over the Gourma (left box) and Fakara (right box) windows. The black crosses locate the field vegetation survey sites over the Gourma region.

4.2.3. Woody cover

The question of the role of the woody cover in the observed re-greening trends has often been raised. To cite just two studies, Herrmann and Tappan (2013) used tree inventory, high resolution imagery and population surveys in central Senegal over the last three decades. They concluded a decline in the high trees population, a strong increase in shrub density, and a decline in species diversity interpreted as a shift towards more arid-tolerant species. Another study based on aerial photography, Ikonos images and field measurements collected in Senegal and Mauritania concluded in a general decline in tree density and diversity in western Sahel (Gonzalez, Tucker, & Sy, 2012). This decreasing tendency was linked to global climate change, through a negative trend in precipitation and an increase in air temperature observed from 1901 to 2002. Some studies however mention an increase of the woody cover over the last decades (Tarchiani, Di Vecchia, Genesio, & Sorani, 2008).

The woody plants population dynamics in the Gourma region have been analyzed through field tree inventories from 1984 to 2006 (Gardelle et al., 2010; Hiernaux, Diarra, et al., 2009). It was shown that, similar to the herbaceous cover, woody plants have a significance resilience to the 1983–84 drought over sandy soils (3.7% in 1985 to 4% in 2006), while a decline is reported over shallow soils (7.8% in 1985 to 3.2% in 2006). In clayed depressions an increase is most often observed, but not everywhere, on average 22% in 1985 and 27% in 2006.

In the Fakara region, it is even more complicated to follow woody cover changes because of the land use dynamics. Broadly, woody cover dynamics is similar to the woody dynamics in Gourma (decline over shallow soils, stable or positive trends over sandy soils), but locally important changes occur because of the land use, like shrub management in cropped fields. Part of the woody cover remains unchanged (agroforestry parks, hedges) while small trees and shrubs growing over fallow areas are cut down when the land becomes cultivated. Therefore, long-term and short-term dynamics are interacting, making it difficult to distinguish a global evolution.

In the Sahel however, productivity is often dominated by annual herbaceous plant productivity (the woody cover being generally lower than 5% of the surface; Sankaran et al., 2005), so that NDVI variability and trends are linked to herbaceous cover dynamics in the first place, as opposed to tree cover. During peak growing season, the radiometric response of woody plants is hardly distinguishable from the herbaceous cover response. Thus, even if the woody cover increased or decreased slightly during the last decades, the influence on the peak growing season NDVI data at the kilometer scale or larger would be difficult to ascribe to changes in tree cover. Because of the phenological lag between herbaceous and woody plants (trees and shrubs leafs remaining green longer), woody plants may be detectable by satellite data mostly at the end of the growing season. The phenological analysis performed in this study showed generally higher trend values during the herbaceous growing season (August and September) than at its end (November).

Based on literature, it seems difficult to find large-scale patterns of woody cover changes, either over pastoral or cultivated lands. More importantly, potential changes in the woody cover that may have taken place in the Sahel are not easily linked to the overall re-greening trends observed during peak growing season, whereas herbaceous productivity, including crops, is a fairly obvious candidate.

4.2.4. Other drivers

Even if the first driver of vegetation productivity remains the rainfall patterns (annual amounts, frequency, redistribution), literature often points out land use, cropping practices in relation with population increase, tree regeneration and improved agro-environmental measures to explain local trends in vegetation productivity and greening trends. Over the agro pastoral Fakara region, a historical increase of areas under cultivation occurred since the 1950s. Because soils in Fakara are poorly fertile and the proportion of arable land is limited, the increase in cropped areas resulted in increasingly cropping marginal lands. In

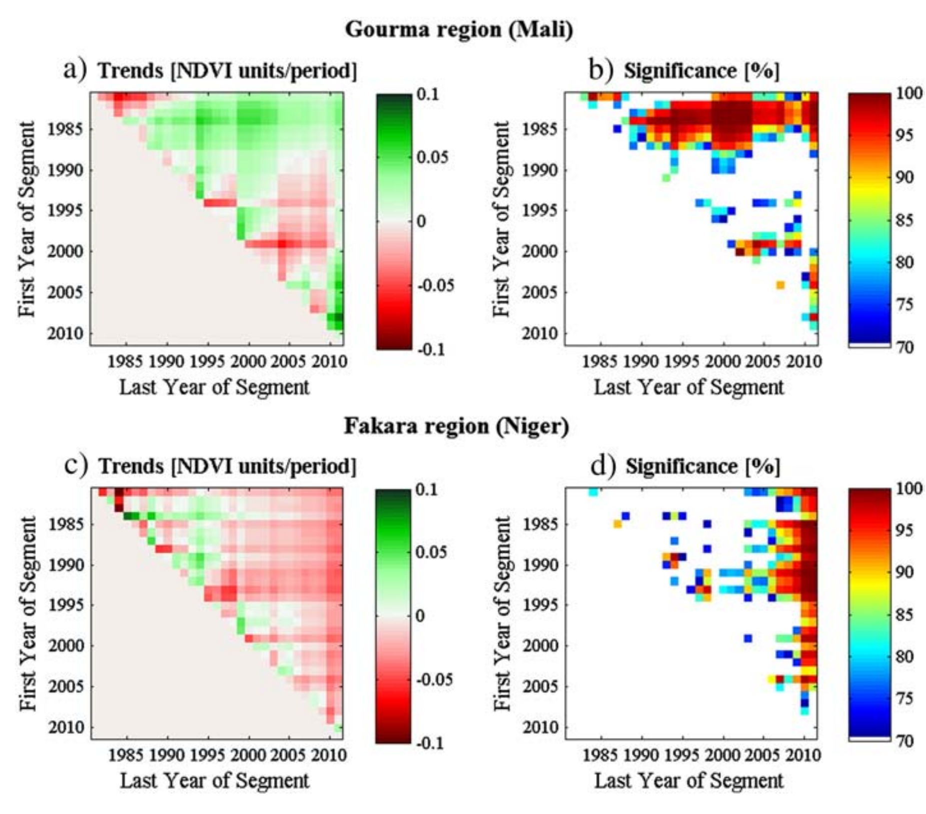

Fig. 8. Sensitivity of the trends to the time period for the Gourma window (a and b) and for the Fakara window (c and d). The left-hand side figures display the NDVI linear increments (a and c), while the right hand side figures display the associated significance values (b and d). The y and x axes are respectively the first and last year of the time period considered. Re-greening trends are in green, negative trends in red. (For interpretation of the references to color in this figure legend, the reader is referred to the web version of this article.)

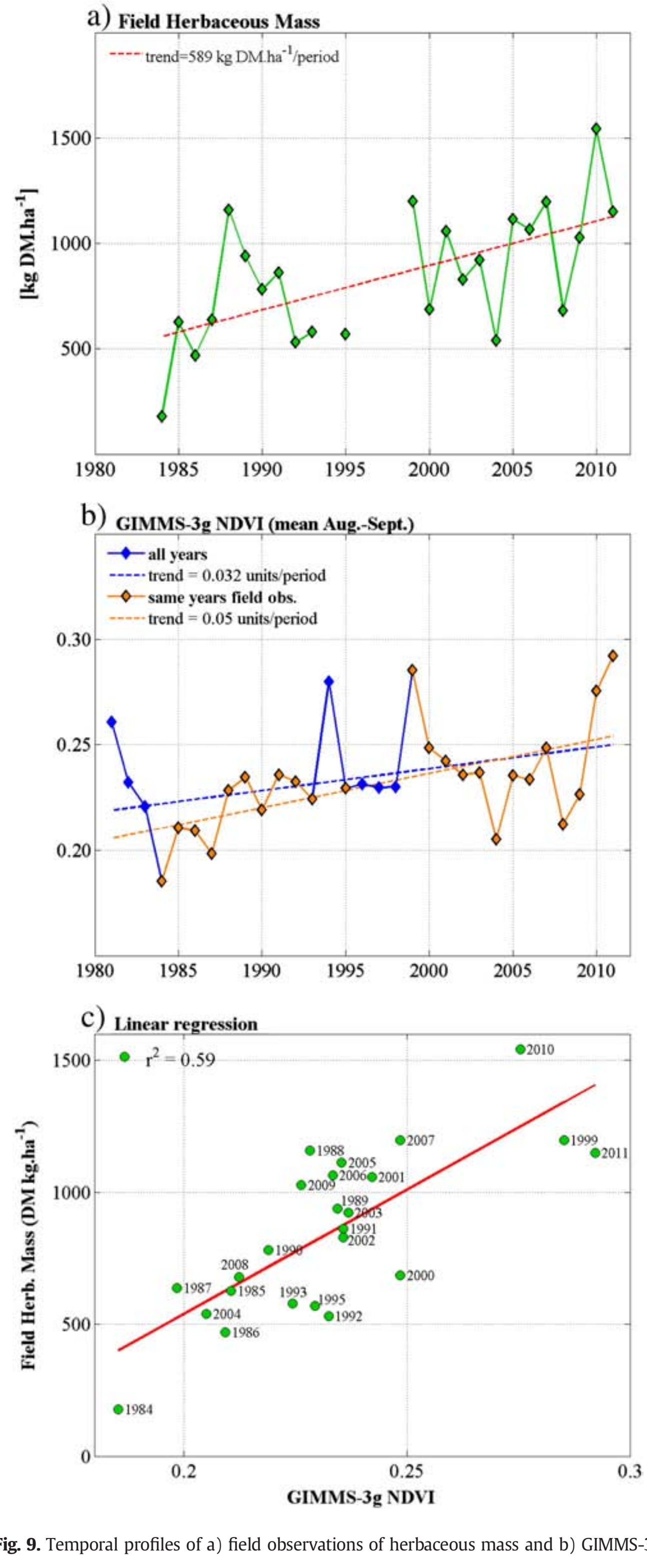

Fig. 9. Temporal profiles of a) field observations of herbaceous mass and b) GIMMS-3g NDVI over the Gourma region. Panel b) shows the NDVI GIMMS-3g for the exact same years when field observations are available (in orange) and for all years when NDVI data are available (1981–2011, in blue). c) Linear regression between GIMMS-3g NDVI and field observations of herbaceous mass over the Gourma window (1984–2011). (For interpretation of the references to color in this figure legend, the reader is referred to the web version of this article.)

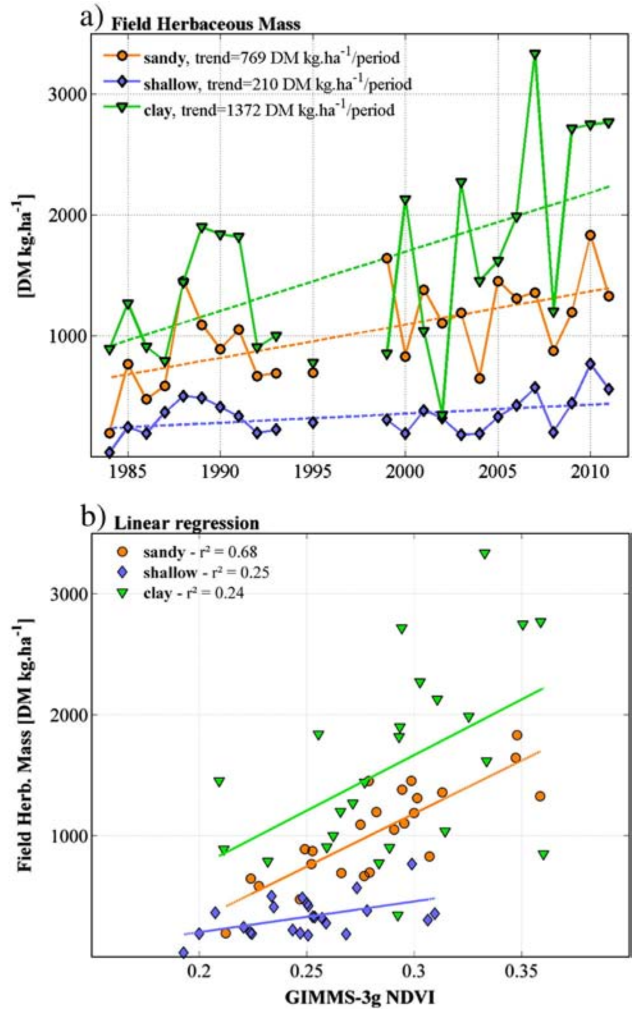

Fig. 10. a) Temporal profiles of field observations of herbaceous mass over the Gourma region. Sites are classified by soil type: sandy soils (circles, orange line), shallow soils (diamonds, blue line) and lowland clay soils (triangles, green line). b) Linear regressions between herbaceous masses and GIMMS-3g NDVI extracted over the corresponding pixel, and aggregated into the three soil type classes (see text for details about the heterogeneity issues). (For interpretation of the references to color in this figure legend, the reader is referred to the web version of this article.)

addition, a reduction in the proportion of fallows has been observed, and a shortening of the fallow duration reported (Hiernaux & Turner, 2002). An increase in the grazing pressure intensity during the rainy season was reported as well, which is related to the cropped areas expansion and thus the reduction of available land for pastoral use (Hiernaux, Diarra, et al., 2009). All these factors might have induced a decline in the "average" (including marginal lands) soil fertility (de Rouw & Rajot, 2004), thus in vegetation productivity, and could explain the persistent decreasing trend in vegetation production observed both by satellite data and field observations of the herbaceous layer. The use of fertilizer and anti-erosion devices in the region is rather limited and does not seem to have a significant impact on the overall decreasing trend.

The constant increase in cropped areas may have changed the relationship between NDVI and the aboveground herbaceous mass over years. In their studies during the HAPEX Sahel experiment in Niger, Hanan, Begue, and Prince (1997) and Hanan, Prince, and Begue (1997) found that seasonal integrated NDVI was higher for fallows than for millet fields when considering aboveground primary production only. They also showed that the efficiency of conversion of intercepted radiation by the canopy into aboveground plant material was higher for millet than for fallow vegetation. Thus, an increase in cropped areas such as the one observed for the Fakara region could result in decreasing NDVI, but not necessarily decreasing aboveground herbaceous mass. On the other hand, Begue et al. (2011) suggested that an increase in cropped areas

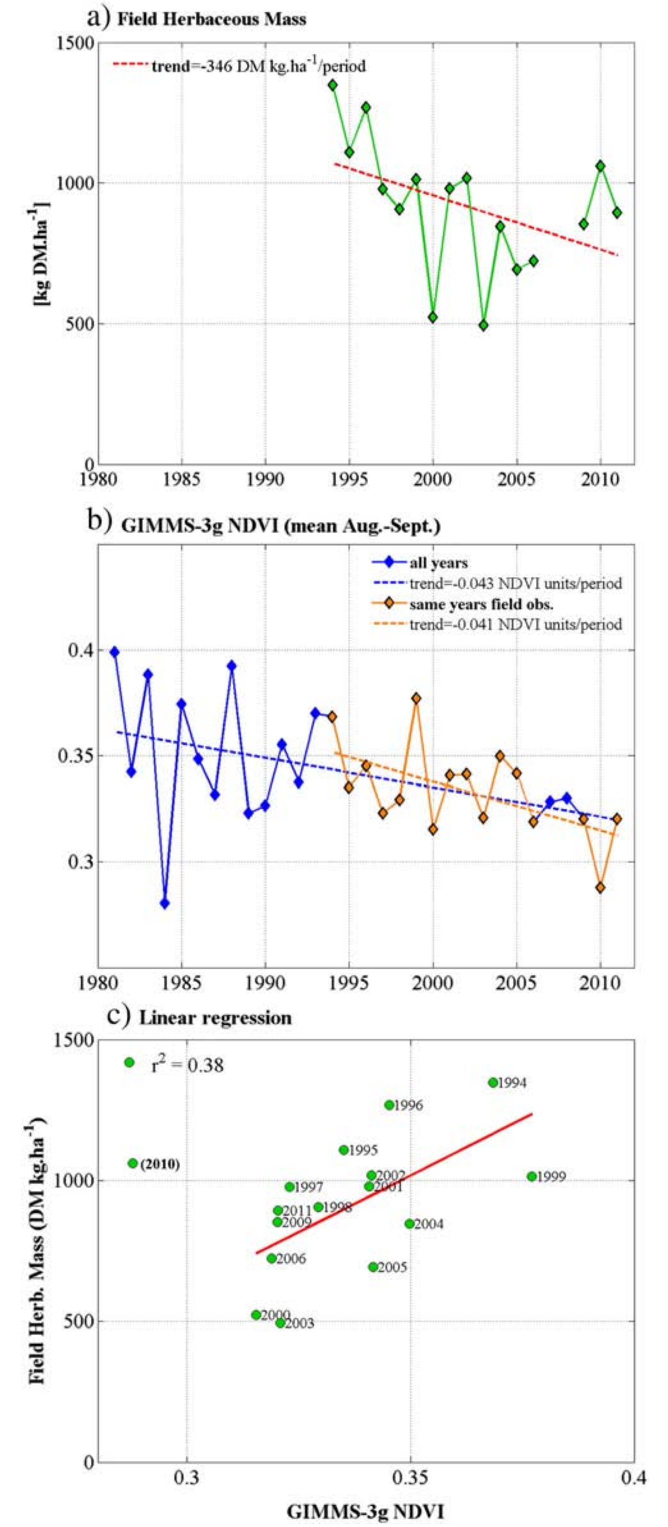

Fig. 11. Temporal profiles of a) field observations of herbaceous mass and b) NDVI GIMMS-3g over the Fakara region. Panel b) shows the NDVI GIMMS-3g for the exact same years when field observations are available (in orange) and for all years when NDVI data are available (1981–2011, in blue). c) Linear regression between field observations of herbaceous mass and GIMMS-3g NDVI over the Fakara region (1994–2011). The regression line is plotted in red (2010 is not considered). (For interpretation of the references to color in this figure legend, the reader is referred to the web version of this article.)

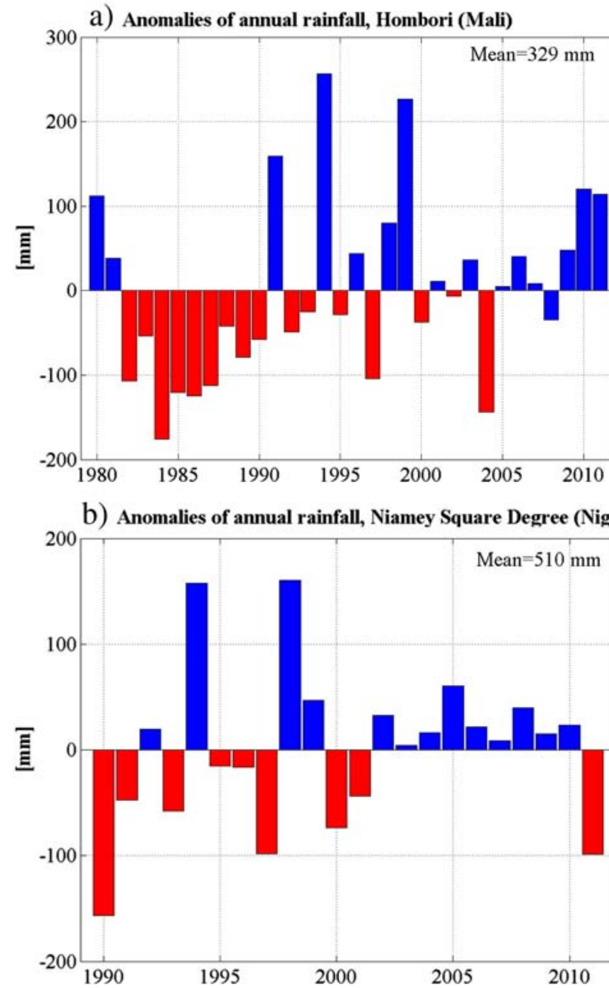

Fig. 12. Anomalies of annual rainfall measured at a) the Hombori meteorological station from 1980 to 2011 and b) over the Niamey Square Degree from 1990 to 2011.
Panel a courtesy of *Direction Nationale de la Météorologie* (DNM) from Mali. Panel b courtesy of AMMA-Catch.

induced an increase in NDVI in their study area in Mali, located in southern Sahel with annual rainfall reaching 700 mm/year. At this stage, it is difficult to conclude about the effect of crop expansion on the overall NDVI signal and on aboveground primary production. Further studies would be required to better understand the changes in the NDVI/mass relationship throughout the time period.

In addition, when the whole Sahel is considered, no systematic correlation between agro-pastoral land use and negative vegetation trends can be observed. Indeed, when looking at the GIMMS-3g NDVI trends over the Sahel, the most intensively cultivated areas such as the groundnut belt in Senegal, Seno in Mali, Yatenga in Burkina Faso, the Haoussa land in northern Nigeria and bordering zone in Niger do not exhibit negative trends, meaning that cropped surface expansion is not systematically associated with negative satellite-observed trends.

5. Conclusion

We analyzed long-term NDVI data together with long-term field observations of vegetation collected in northern Mali and western Niger from 1984 to 2011 and from 1994 to 2011 respectively. A good agreement was found between NDVI and field measurements of the herbaceous layer mass, both for the Gourma and Fakara regions, where positive and negative trends were found respectively. Thus, the GIMM3g archives revealed consistent over time and well correlated to trends in vegetation productivity over the whole 1981–2011 period.

The re-greening trends observed over pastoral Gourma were found highly significant over the whole period, and particularly so when including the years following the 1983–84 drought. This implies a significant resilience of Sahelian ecosystems to extreme climatic events. Soil type and soil depth were found to significantly modulate the vegetation trends observed. Indeed, positive vegetation trends were found over the widespread deep sandy soils, while non-significant trends in vegetation cover were observed over shallow soils. In the agro-pastoral Fakara re-greening patterns were only found immediately after the drought and a constant decline in NDVI was observed starting in the mid 1990s that could not be related to rainfall. Several factors may be responsible for this decline in productivity, such as the historical increase in cropped areas, changes in land use, a shortening of the fallow duration, an increase in the grazing pressure intensity during the rainy season, and a decline in soil fertility.

For the whole Sahel, the satellite greening trend is dominant, and the present analysis points toward a large-scale increase of herbaceous production over 1981–2011, and a less important role of degradation either because of it is less common or because the changes occur at a smaller spatial scale than the satellite products' resolution.

In addition to proving the consistency of multi-sensor satellite time-series, this study shows that greening is associated with increasing herbaceous productivity. It also shows that 'browning' occurs, both in satellite series and field observations, which helps reconciling the re-greening and desertification theories.

Acknowledgments

We are thankful to the two reviewers for their helpful comments which contributed to improve this manuscript. Dardel C. is supported by CNES. Support from AMMA-Catch, ANR ESCAPE (ANR-10-CEPL-005) and AMMA-IP are also acknowledged. Precipitation data are kindly provided by DNM Mali and Niger. We are grateful to the GIMMS group for their ongoing efforts and for sharing their NDVI3g data. Finally, we thank all the people who participated to the field surveys over this 28-year long period!

References

An, N., Price, K. P., & Blair, J. M. (2013). Estimating above-ground net primary productivity of the tallgrass prairie ecosystem of the Central Great Plains using AVHRR NDVI. *International Journal of Remote Sensing*, *34*, 3717–3735.

Anyamba, A., & Tucker, C. J. (2005). Analysis of Sahelian vegetation dynamics using NOAA-AVHRR NDVI data from 1981–2003. *Journal of Arid Environments*, *63*, 596–614.

Aubreville, A., & Chevalier, A. (1949). *Climats, forêts et désertification de l'Afrique tropicale*. Paris: Société d'éd. géographiques, maritimes et coloniales (351 pages).

Beck, H. E., McVicar, T. R., van Dijk, A., Schellekens, J., de Jeu, R. A.M., & Bruijnzeel, L. A. (2011). Global evaluation of four AVHRR-NDVI data sets: Intercomparison and assessment against Landsat imagery. *Remote Sensing of Environment*, *115*, 2547–2563.

Begue, A., Vintrou, E., Ruelland, D., Claden, M., & Dessay, N. (2011). Can a 25-year trend in Soudano-Sahelian vegetation dynamics be interpreted in terms of land use change? A remote sensing approach. *Global Environmental Change—Human and Policy Dimensions*, *21*, 413–420.

Boudet, G. (1972). *Désertification de l'Afrique tropicale sèche. Adansonia. Série 2*, *12*. (pp. 505–524), 505–524.

Boudet, G. (1977). *Désertification ou remontée biologique du Sahel. Cahiers ORSTOM. Série Biologie: Ecologie et Biologie Végétale*, *12*. (pp. 293–300), 293–300.

Cappelaere, B., Descroix, L., Lebel, T., Boulain, N., Ramier, D., Laurent, J. P., et al. (2009). The AMMA-CATCH experiment in the cultivated Sahelian area of south-west Niger: Investigating water cycle response to a fluctuating climate and changing environment. *Journal of Hydrology*, *375*, 34–51.

Charney, J. G. (1975). Dynamics of deserts and drought in Sahel. *Quarterly Journal of the Royal Meteorological Society*, *101*, 193–202.

Cottam, G., & Curtis, J. T. (1956). The use of distance measures in phytosociological sampling. *Ecology*, *37*, 451–460.

de Jong, R., de Bruin, S., de Wit, A., Schaepman, M. E., & Dent, D. L. (2011). Analysis of monotonic greening and browning trends from global NDVI time-series. *Remote Sensing of Environment*, *115*, 692–702.

de Rouw, A., & Rajot, J. L. (2004). Nutrient availability and pearl millet production in Sahelian farming systems based on manuring or fallowing. *Agriculture, Ecosystems & Environment*, *104*, 249–262.

Descroix, L., Laurent, J. P., Vauclin, M., Amogu, O., Boubkraoui, S., Ibrahim, B., et al. (2012). Experimental evidence of deep infiltration under sandy flats and gullies in the Sahel. *Journal of Hydrology*, *424*, 1–15.

Descroix, L., Mahe, G., Lebel, T., Favreau, G., Galle, S., Gautier, E., et al. (2009). Spatio-temporal variability of hydrological regimes around the boundaries between Sahelian and Sudanian areas of West Africa: A synthesis. *Journal of Hydrology*, *375*, 90–102.

Diallo, O., Diouf, A., Hanan, N.P., Ndiaye, A., & Prevost, Y. (1991). AVHRR monitoring of savanna primary production in Senegal, West Africa — 1987–1988. *International Journal of Remote Sensing*, *12*, 1259–1279.

Eklundh, L., & Olsson, L. (2003). Vegetation index trends for the African Sahel 1982–1999. *Geophysical Research Letters*, *30*, 1430–1433.

Fensholt, R., Langanke, T., Rasmussen, K., Reenberg, A., Prince, S. D., Tucker, C., et al. (2012). Greenness in semi-arid areas across the globe 1981–2007 — an Earth Observing Satellite based analysis of trends and drivers. *Remote Sensing of Environment*, *121*, 144–158.

Fensholt, R., & Rasmussen, K. (2010). Analysis of trends in the Sahelian 'rain-use efficiency' using GIMMS NDVI, RFE and GPCP rainfall data. *Remote Sensing of Environment*, *115*, 438–451.

Fensholt, R., Rasmussen, K., Nielsen, T. T., & Mbow, C. (2009). Evaluation of earth observation based long term vegetation trends — Inter-comparing NDVI time series trend analysis consistency of Sahel from AVHRR GIMMS, Terra MODIS and SPOT VGT data. *Remote Sensing of Environment*, *113*, 1886–1898.

Fensholt, R., Sandholt, I., & Stisen, S. (2006). Evaluating MODIS, MERIS, and VEGETATION — Vegetation indices using *in situ* measurements in a semiarid environment. *IEEE Transactions on Geoscience and Remote Sensing*, *44*, 1774–1786.

Fensholt, R., Sandholt, I., Stisen, S., & Tucker, C. (2006). Analysing NDVI for the African continent using the geostationary meteosat second generation SEVIRI sensor. *Remote Sensing of Environment*, *101*, 212–229.

Gardelle, J., Hiernaux, P., Kergoat, L., & Grippa, M. (2010). Less rain, more water in ponds: A remote sensing study of the dynamics of surface waters from 1950 to present in pastoral Sahel (Gourma region, Mali). *Hydrology and Earth System Sciences*, *14*, 309–324.

Gonzalez, P., Tucker, C. J., & Sy, H. (2012). Tree density and species decline in the African Sahel attributable to climate. *Journal of Arid Environments*, *78*, 55–64.

Hanan, N.P., Begue, A., & Prince, S. D. (1997). Errors in remote sensing of intercepted photosynthetically active radiation: An example from HAPEX-Sahel. *Journal of Hydrology*, *189*, 676–696.

Hanan, N.P., Prince, S. D., & Begue, A. (1997). Modelling vegetation primary production during HAPEX-Sahel using production efficiency and canopy conductance model formulations. *Journal of Hydrology*, *189*, 651–675.

Hein, L., & de Ridder, N. (2006). Desertification in the Sahel: A reinterpretation. *Global Change Biology*, *12*, 751–758.

Hellden, U. (1991). Desertification — Time for an assessment. *Ambio*, *20*, 372–383.

Hellden, U., & Tottrup, C. (2008). Regional desertification: A global synthesis. *Global and Planetary Change*, *64*, 169–176.

Herrmann, S. M., Anyamba, A., & Tucker, C. J. (2005). Recent trends in vegetation dynamics in the African Sahel and their relationship to climate. *Global Environmental Change—Human and Policy Dimensions*, *15*, 394–404.

Herrmann, S. M., & Tappan, G. G. (2013). Vegetation impoverishment despite greening: A case study from central Senegal. *Journal of Arid Environments*, *90*, 55–66.

Heumann, B. W., Seaquist, J. W., Eklundh, L., & Jonsson, P. (2007). AVHRR derived phenological change in the Sahel and Soudan, Africa, 1982–2005. *Remote Sensing of Environment*, *108*, 385–392.

Hickler, T., Eklundh, L., Seaquist, J. W., Smith, B., Ardo, J., Olsson, L., et al. (2005). Precipitation controls Sahel greening trend. *Geophysical Research Letters*, *32*, L21415.

Hiernaux, P. (1988). Vegetation monitoring by remote sensing: progress in calibrating a radiometric index and its application in the Gourma, Mali. *ILCA Bulletin*, *32*, 14–21 (available from http://www.ilri.org/InfoServ/Webpub/fulldocs/Bulletin32/vegeta.htm)

Hiernaux, P., & Ayantunde, A. (2004). The Fakara: A semi-arid agro-ecosystem under stress. *Report of research activities, first phase (July 2002–June 2004) of the DMP-GEF Program (GEF/2711-02-4516)*. Nairobi (Kenya): ILRI (available from http://hdl.handle.net/10568/1550)

Hiernaux, P., Ayantunde, A., Kalilou, A., Mougin, E., Gerard, B., Baup, F., et al. (2009). Trends in productivity of crops, fallow and rangelands in Southwest Niger: impact of land use, management and variable rainfall. *Journal of Hydrology*, *375*, 65–77.

Hiernaux, P., Diarra, L., Trichon, V., Mougin, E., Soumaguel, N., & Baup, F. (2009). Woody plant population dynamics in response to climate changes from 1984 to 2006 in Sahel (Gourma, Mali). *Journal of Hydrology*, *375*, 103–113.

Hiernaux, P., Mougin, E., Diarra, L., Soumaguel, N., Lavenu, F., Tracol, Y., et al. (2009). Sahelian rangeland response to changes in rainfall over two decades in the Gourma region, Mali. *Journal of Hydrology*, *375*, 114–127.

Hiernaux, P., & Turner, M.D. (1996). The effect of clipping on growth and nutrient uptake of Sahelian annual rangelands. *Journal of Applied Ecology*, *33*, 387–399.

Hiernaux, P., & Turner, M.D. (2002). The influence of farmer and pastoralist management practices on desertification processes in the Sahel. In J. F. Reynolds, & D.M. Stafford Smith (Eds.), *Global desertification: Do humans cause deserts?* (pp. 35–148). Berlin: Dahlem University Press.

Holben, B. N. (1986). Characteristics of maximum-value composite images from temporal AVHRR data. *International Journal of Remote Sensing*, *7*, 1417–1434.

Huber, S., Fensholt, R., & Rasmussen, K. (2011). Water availability as the driver of vegetation dynamics in the African Sahel from 1982 to 2007. *Global and Planetary Change*, *76*, 186–195.

Hubert, H. (1920). Le dessèchement progressif en Afrique occidentale. *Bulletin du Comité d'études Historiques et Scientifiques de l'Afrique Occidentale Française*, *3*, 401–467.

Hulme, M. (2001). Climatic perspectives on Sahelian desiccation: 1973–1998. *Global Environmental Change—Human and Policy Dimensions*, *11*, 19–29.

Hutchinson, C. F., Herrmann, S. M., Maukonen, T., & Weber, J. (2005). Introduction: The "greening" of the Sahel. *Journal of Arid Environments*, *63*, 535–537.

James, M. E., & Kalluri, S. N. V. (1994). The Pathfinder AVHRR land data set — An improved coarse resolution data set for terrestrial monitoring. *International Journal of Remote Sensing*, *15*, 3347–3363.

Jones, B. (1938). Desiccation and the West African colonies. *Geographical Journal*, *91*, 401–423.

Justice, C. O., Townshend, J. R. G., Vermote, E. F., Masuoka, E., Wolfe, R. E., Saleous, N., et al. (2002). An overview of MODIS Land data processing and product status. *Remote Sensing of Environment*, *83*, 3–15.

Justice, C. O., Vermote, E., Townshend, J. R. G., Defries, R., Roy, D. P., Hall, D. K., et al. (1998). The Moderate Resolution Imaging Spectroradiometer (MODIS): Land remote sensing for global change research. *IEEE Transactions on Geoscience and Remote Sensing*, *36*, 1228–1249.

Kidwell, K. B. (1998). *NOAA polar orbiters user's guide*. National Oceanic and Atmospheric Administration. Washington, D.C.: U.S. Department of Commerce, 20–233.

Le Barbé, L., & Lebel, T. (1997). Rainfall climatology of the HAPEX-Sahel region during the years 1950–1990. *Journal of Hydrology*, *189*, 43–73.

Le Houerou, H. N. (1984). Rain use efficiency — A unifying concept in arid-land ecology. *Journal of Arid Environments*, *7*, 213–247.

Le Houerou, H. N. (1996). Climate change, drought and desertification. *Journal of Arid Environments*, *34*, 133–185.

Lebel, T., & Ali, A. (2009). Recent trends in the Central and Western Sahel rainfall regime (1990–2007). *Journal of Hydrology*, *375*, 52–64.

Lindqvist, S., & Tengberg, A. (1993). New evidence of desertification from case-studies in northern Burkina-Faso. *Geografiska Annaler, Series A: Physical Geography*, *75*, 127–135.

Los, S. O. (1998). Estimation of the ratio of sensor degradation between NOAA AVHRR channels 1 and 2 from monthly NDVI composites. *IEEE Transactions on Geoscience and Remote Sensing*, *36*, 206–213.

Mbow, C., Fensholt, R., Rasmussen, K., & Diop, D. (2013). Can vegetation productivity be derived from greenness in a semi-arid environment? Evidence from ground-based measurements. *Journal of Arid Environments*, *97*, 56–65.

Mougin, E., Hiernaux, P., Kergoat, L., Grippa, M., de Rosnay, P., Timouk, F., et al. (2009). The AMMA-CATCH Gourma observatory site in Mali: Relating climatic variations to changes in vegetation, surface hydrology, fluxes and natural resources. *Journal of Hydrology*, *375*, 14–33.

Myneni, R. B., Hall, F. G., Sellers, P. J., & Marshak, A. L. (1995). The interpretation of spectral vegetation indexes. *IEEE Transactions on Geoscience and Remote Sensing*, *33*, 481–486.

Myneni, R. B., & Williams, D. L. (1994). On the relationship between FAPAR and NDVI. *Remote Sensing of Environment*, *49*, 200–211.

Nicholson, S. E. (2013). *The West African Sahel: A review of recent studies on the rainfall regime and its interannual variability*. *ISRN Meteorology*, *Vol. 2013*, http://dx.doi.org/10.1155/2013/453521 (Article ID 453521).

Nicholson, S. E., & Palao, I. M. (1993). A reevaluation of rainfall variability in the Sahel. 1. Characteristics of rainfall fluctuations. *International Journal of Climatology*, *13*, 371–389.

Nicholson, S. E., Tucker, C. J., & Ba, M. B. (1998). Desertification, drought, and surface vegetation: An example from the West African Sahel. *Bulletin of the American Meteorological Society*, *79*, 815–829.

Olsson, L., Eklundh, L., & Ardo, J. (2005). A recent greening of the Sahel — Trends, patterns and potential causes. *Journal of Arid Environments*, *63*, 556–566.

Pedelty, J., Devadiga, S., Masuoka, E., Brown, M., Pinzon, J., Tucker, C. J., et al. (2007). Generating a long-term land data record from the AVHRR and MODIS instruments. *IGARSS 2007. Sensing and understanding our planet*, *Vol. 1–12*. (pp. 1021–1024). New York: IEEE.

Penning de Vries, F. W. T., & Djitéye, M.A. (1982). *La Productivité des pâturages sahéliens: une étude des sols, des végétations et de l'exploitation de cette ressource naturelle*. Wageningen: Centre for Agricultural Pub. and Documentation.

Pinzon, J. E., Brown, M. E., & Tucker, C. J. (2005). *EMD correction of orbital drift artifacts in satellite data stream*. Hilbert–Huang transform and its applications. Singapore: World Scientific Publ Co Pte Ltd, 167–186.

Prince, S. D. (1991). Satellite remote-sensing of primary production — Comparison of results for Sahelian grasslands 1981–1988. *International Journal of Remote Sensing*, *12*, 1301–1311.

Prince, S. D., De Colstoun, E. B., & Kravitz, L. L. (1998). Evidence from rain-use efficiencies does not indicate extensive Sahelian desertification. *Global Change Biology*, *4*, 359–374.

Prince, S. D., Wessels, K. J., Tucker, C. J., & Nicholson, S. E. (2007). Desertification in the Sahel: A reinterpretation of a reinterpretation. *Global Change Biology*, *13*, 1308–1313.

Sala, O. E., & Austin, A. T. (2000). Methods of estimating aboveground net primary productivity. In O. E. Sala, R. B. Jackson, H. A. Mooney, & R. W. Howarth (Eds.), *Methods in ecosystem science* (pp. 31–43). New-York: Springer.

Sankaran, M., Hanan, N.P., Scholes, R. J., Ratnam, J., Augustine, D. J., Cade, B.S., et al. (2005). Determinants of woody cover in African savannas. *Nature*, *438*, 846–849.

Seaquist, J. W., Hickler, T., Eklundh, L., Ardo, J., & Heumann, B. W. (2009). Disentangling the effects of climate and people on Sahel vegetation dynamics. *Biogeosciences*, *6*, 469–477.

Stebbing, E. P. (1935). The encroaching Sahara: The threat to the West African colonies. *Geographical Journal*, *85*, 506–524.

Tarchiani, V., Di Vecchia, A., Genesio, L., & Sorani, F. (2008). Monitoring drylands ecosystem dynamics for sustainable development policies: The Keita experience. In C. Lee, & T. Schaaf (Eds.), *The future of Drylands* (pp. 395–407). : UNESCO.

Timouk, F., Kergoat, L., Mougin, E., Lloyd, C. R., Ceschia, E., Cohard, J. M., et al. (2009). Response of surface energy balance to water regime and vegetation development in a Sahelian landscape. *Journal of Hydrology*, *375*, 178–189.

Townshend, J. R. G., & Justice, C. O. (1995). Spatial variability of images and the monitoring of changes in the Normalized Difference Vegetation Index. *International Journal of Remote Sensing*, *16*, 2187–2195.

Tucker, C. J. (1979). Red and photographic infrared linear combinations for monitoring vegetation. *Remote Sensing of Environment*, *8*, 127–150.

Tucker, C. J., Dregne, H. E., & Newcomb, W. W. (1991). Expansion and contraction of the Sahara desert from 1980 to 1990. *Science*, *253*, 299–301.

Tucker, C. J., Justice, C. O., & Prince, S. D. (1986). Monitoring the grasslands of the Sahel 1984–1985. *International Journal of Remote Sensing*, *7*, 1571–1581.

Tucker, C. J., Newcomb, W. W., & Dregne, H. E. (1994). AVHRR data sets for determination of desert spatial extent. *International Journal of Remote Sensing*, *15*, 3547–3565.

Tucker, C. J., & Nicholson, S. E. (1999). Variations in the size of the Sahara desert from 1980 to 1997. *Ambio*, *28*, 587–591.

Tucker, C. J., Pinzon, J. E., Brown, M. E., Slayback, D. A., Pak, E. W., Mahoney, R., et al. (2005). An extended AVHRR 8-km NDVI dataset compatible with MODIS and SPOT vegetation NDVI data. *International Journal of Remote Sensing*, *26*, 4485–4498.

Tucker, C. J., Vanpraet, C. L., Sharman, M. J., & Van Ittersum, G. (1985). Satellite remote-sensing of total herbaceous biomass production in the Senegalese Sahel — 1980–1984. *Remote Sensing of Environment*, *17*, 233–249.

Vermote, E., & Kaufman, Y. J. (1995). Absolute calibration of AVHRR visible and near-infrared channels using ocean and cloud views. *International Journal of Remote Sensing*, *16*, 2317–2340.

Zhu, Z. C., Bi, J., Pan, Y. Z., Ganguly, S., Anav, A., Xu, L., et al. (2012). Global Data Sets of Vegetation Leaf Area Index (LAI)3g and Fraction of Photosynthetically Active Radiation (FPAR)3g derived from Global Inventory Modeling and Mapping Studies (GIMMS) Normalized Difference Vegetation Index (NDVI3g) for the period 1981 to 2011. *Remote Sensing*, *5*, 927–948.